

Peer review status:

This is a non-peer-reviewed preprint submitted to EarthArXiv.

1     **Adaptive Turbine Replacement Improves Hydropower**  
2             **Flexibility in a Changing Climate**

3             **Veysel Yildiz<sup>1</sup>, Nathalie Voisin<sup>2,3</sup>, and Marta Zaniolo<sup>1</sup>**

4             <sup>1</sup>Department of Civil and Environmental Engineering, Duke University, NC, USA

5                     <sup>2</sup>Pacific Northwest National Laboratory, WA, USA

6                             <sup>3</sup>University of Washington, WA, USA

7             **Key Points:**

- 8             • HyTUNE identifies optimal turbine retrofit strategies that maximize performance  
9                 and economic value under changing hydrologic conditions.
- 10            • Proactive, adaptive turbine replacements reduce efficiency losses from aging and  
11                 variable operations, increasing firm power and peak capacity.
- 12            • The framework strengthens resilience to drought and hydrologic extremes by sus-  
13                 taining performance and economic returns at low reservoir levels.

---

Corresponding author: Veysel Yildiz, [veysel.yildiz@duke.edu](mailto:veysel.yildiz@duke.edu)

**Abstract**

Hydropower Plants (HP) will operate under new conditions as water regimes shift, reservoir operating rules evolve, and the grid requires flexible balancing of wind and solar. HP turbine systems are traditionally designed to operate at the highest efficiency within narrow ranges of flow and reservoir levels while deviations from design conditions can degrade HP efficiency and trigger failures, especially in aging infrastructure. Turbine replacements typically occur every 35 to 50 years, offering a rare opportunity to modernize turbine designs by adjusting turbine head and discharge capacity to fit new conditions, rather than replicating legacy designs. The central challenge is to determine when to replace instead of extending lifetime of existing fleet, which system signals indicate the need for redesign, and which configurations will deliver the most robust gains.

This study introduces HyTUNE (Hydropower Turbine Upgrade and Next-generation Planning), a dynamic decision-support tool that integrates basin hydrology, plant hydraulics, and adaptive optimization to guide turbine replacement timing and configuration. HyTUNE shifts planning from reactive, end-of-life replacement toward proactive, information-driven strategies. The framework learns from evolving system states, identifies threshold conditions where adjustments in head or capacity improve performance, and prescribes phased interventions that balance energy production, reliability, and cost under uncertainty. Application to the Hoover Hydropower Plant demonstrates that HyTUNE’s adaptive policies consistently outperformed conventional reactive strategies across diverse hydrologic futures. HyTUNE is of considerable practical relevance as hydropower systems worldwide confront the dual challenge of modernization and adaptation to future uncertainty and demand growth.

**1 Introduction**

Hydropower is a key renewable energy source that provides large-scale, low-carbon electricity and supports the transition to decarbonized energy systems (Hertwich et al., 2016). Reservoir-based hydropower systems are expected to play an increasing role in the future grid, not only through reliable generation but also by acting as large-scale batteries that supply electricity on demand. This flexibility helps balance variable renewable sources such as wind and solar, maintaining grid stability as renewable penetration grows (H. Liu et al., 2019; Owolabi et al., 2022; Fälth et al., 2025).

45 Despite this central role, hydropower plant (HP) design has remained largely un-  
46 changed for decades. Designing a HP requires selecting an optimal turbine configura-  
47 tion, including the number of turbines, their discharge capacity, and head. This design  
48 is typically aimed at energy production efficiency within nominal hydrological "design"  
49 conditions, namely a narrow range of reservoir level and release (Kaunda et al., 2014;  
50 Singh & Singal, 2017; Kincic et al., 2022; Yildiz et al., 2024), while also aiming to sim-  
51 plify maintenance and operations (Witt et al., 2017; Amougou et al., 2022; Bisnett et  
52 al., 2022). The result is a uniform configuration of turbines at one plant, where identi-  
53 cal turbines operate under the same head and capacity (e.g., M. M. Johnson, 2024; Quar-  
54 anta & Hunt, 2022). While such systems yield very high efficiency within their design  
55 conditions (ESHA, 2004; USBR, 2011; X. Liu et al., 2015; Yildiz & Vrugt, 2019; Muntean  
56 et al., 2016; Mikhailov et al., 2021), efficiency declines sharply outside these conditions  
57 when reservoir levels fall below the design head, or releases become more variable. En-  
58 ergy production may have to stop altogether when reservoir head falls below the min-  
59 imum design head. A loss in efficiency not only means that less energy is generated per  
60 unit of water released, but it also often leads to increased mechanical wear and opera-  
61 tional challenges (Diaz et al., 2010; Dorji & Ghomashchi, 2014; Celebioglu et al., 2017;  
62 Quaranta et al., 2021).

63 Operating reservoir-based hydropower within its high-efficiency design range is be-  
64 coming increasingly challenging. Shifts in water availability, energy demand, and oper-  
65 ating constraints now push plants beyond the conditions for which they were designed.  
66 First, climate change is altering watershed hydrology, increasing variability in inflows and  
67 reservoir levels (Schaeffer et al., 2012; Van Vliet et al., 2016; Ramião et al., 2023). More  
68 frequent and severe droughts often lower reservoir water levels below design head, reduc-  
69 ing efficiency or halting production. For example, California's Hyatt Hydropower Plant  
70 stopped generating in 2021 when record-low levels in Lake Oroville fell below the oper-  
71 ational head (Kincic et al., 2022). Even less extreme conditions cause cumulative losses.  
72 Recent studies report a nationwide decline in hydropower capacity factors, largely driven  
73 by changing hydrologic regimes (Turner et al., 2024). The steepest reductions were recorded  
74 in the Pacific Northwest, California, and the Colorado River Basin. For example, climate  
75 variability explains more than 80 % of the observed decline in capacity factor of every  
76 major facility in the Colorado River Basin.

77           Second, the role of hydropower in the energy grid is evolving as the share of vari-  
78           able renewable energy increases. As countries pursue net-zero targets, wind and solar  
79           generation are growing rapidly due to falling costs, technological advances, and policy  
80           incentives (Carlino et al., 2023; Hassan et al., 2024). While essential for decarbonization,  
81           their production is inherently variable and non-dispatchable, increasing the risk of fre-  
82           quency instability (Gernaat et al., 2021; Smolarz et al., 2023; L. Liu et al., 2023; Sun et  
83           al., 2024). Hydropower is uniquely positioned to offer stabilizing services to the grid, of-  
84           fering rapid ramping capabilities that allow plants to adjust output quickly in response  
85           to fluctuations in demand or renewable supply (Egré & Milewski, 2002; Sternberg, 2010;  
86           Zhou et al., 2015; Emmanuel et al., 2020). In grids with high renewable shares, hydropower  
87           operations are increasingly constrained by the need to balance variable demand and sup-  
88           ply patterns (De Silva et al., 2022; Datta et al., 2022; Arnold et al., 2024). These con-  
89           ditions often force plants to operate outside their optimal efficiency range (Turner et al.,  
90           2024). A recent study reported a 4 % decline in simulated generation due to efficiency  
91           losses when hydropower complemented wind and solar output (Q. Cheng et al., 2023).

92           Third, reservoir-based HP operations are evolving to meet shifting energy and wa-  
93           ter demands for agriculture, urban use, and ecosystem services, introducing new tem-  
94           poral and spatial challenges for water allocation (Huang et al., 2021; Mishra et al., 2021;  
95           Yildiz et al., 2022; M. Cheng et al., 2022). At the same time, stricter environmental flow  
96           requirements further constrain releases (Ramulifho et al., 2019; Cameron & Pracheil, 2022;  
97           Widén et al., 2024). These trends are driving a shift toward flexible reservoir manage-  
98           ment, where levels and releases vary to balance competing needs rather than staying within  
99           the narrow conditions that maximize turbine efficiency.

100           One promising strategy to expand operational flexibility is the use of heterogeneous  
101           turbine setups, where turbines operate at different heads and capacities (Sample et al.,  
102           2015; Mikhailov et al., 2021; Brown et al., 2024; Yildiz et al., 2025a). Such configura-  
103           tions broaden the range of efficient operation by matching turbine design to expected  
104           hydrologic and grid conditions. In reservoirs projected to experience declining water lev-  
105           els, lower-head turbines can sustain generation as storage decreases. In energy systems  
106           with high renewable penetration, larger-capacity turbines can improve the ability to pro-  
107           vide peaking, ramping, and inertia services while maintaining overall efficiency. Although  
108           heterogeneous setups may slightly reduce maximum efficiency, they increase mean effi-  
109           ciency across a wider operating range, making them particularly valuable in systems un-

110 dergoing change. Real-world examples remain rare. During the recent drought in the Col-  
111 orado River Basin, Hoover Dam replaced five of its seventeen turbines with lower-head  
112 models to maintain production under reduced reservoir levels (Farmer, 2020). Similarly,  
113 Conowingo Hydropower Plant in Maryland and Comerford in New Hampshire added smaller  
114 units to generate power from environmental flow releases (March & Jacobson, 2016). A  
115 nationwide assessment of more than 200 U.S. facilities estimated that installing environmental-  
116 flow turbines could add 730 MW of capacity and produce nearly 1.8 TWh of additional  
117 energy each year (Garrett et al., 2023).

118 Hydropower turbines typically require replacement every 35 to 50 years (International  
119 Energy Agency, 2021; Quaranta & Hunt, 2022). Each refurbishment is a multimillion-  
120 dollar intervention that shapes system reliability and generation capacity for decades.  
121 In the US, many facilities will reach refurbishment age within the next decade, creat-  
122 ing a narrow window to reconsider turbine selection and plant configuration in light of  
123 shifting hydrologic regimes and operating constraints. Yet until now, most turbine re-  
124 placements still replicate the existing design (e.g., M. M. Johnson, 2024; Quaranta & Hunt,  
125 2022; Papillon & Freeman, 2013; Morgado et al., 2020). Upgrades often focus on newer  
126 turbine models that incorporate incremental mechanical improvements relative to the  
127 retired units (IRENA, 2012; Mikhailov et al., 2021) that yield slight efficiency gains (Muntean  
128 et al., 2016; Quaranta et al., 2021), but the overall system configuration typically remains  
129 unchanged.

130 We currently lack decision-support frameworks to determine the optimal timing  
131 and configuration of turbine retrofits under changing hydrology. Existing predictive main-  
132 tenance tools, including the U.S. Bureau of Reclamation’s HydroAMP system (Neijens  
133 & Hayes, 2017), focus on mechanical failure risk (Shanbhag et al., 2025) but do not con-  
134 sider climate uncertainty, evolving operational constraints, or long-term retrofit optimiza-  
135 tion.

136 A proactive framework should inform operators to determine two key decisions: when  
137 to replace or upgrade turbines (or, conversely, when to extend the lifetime of existing fleet),  
138 and which configurations best enhance system resilience to hydrologic and operational  
139 variability. We introduce HyTUNE (Hydropower Turbine Upgrade and Next-generation  
140 Planning), a dynamic decision-support tool that integrates basin-scale hydrology and plant  
141 hydraulics within a control framework. HyTUNE tracks variables such as reservoir level,

142 inflow, and turbine efficiency to identify when replacement is optimal. For each inter-  
143 vention, it specifies the number of turbines to replace and the ideal head and capacity  
144 for the new configuration. The framework also incorporates regulatory and institutional  
145 constraints; for example, upgrades that increase capacity by less than 15 % can avoid  
146 triggering re-licensing requirements in the United States (A. Levine et al., 2017; Sensiba  
147 & McCormick, 2021). The system is trained and tested across a broad ensemble of hy-  
148 drologic scenarios to ensure robustness under uncertainty.

149 We apply this framework to the Hoover Hydropower Plant, a system that has re-  
150 cently experienced significant hydrologic variability and turbine retrofits in response to  
151 declining reservoir levels. Using HyTUNE, we explore how a proactive, data-driven ap-  
152 proach to turbine replacement can guide future modernization under projected climate  
153 and operational uncertainty. The analysis benchmarks HyTUNE’s optimized replacement  
154 policy against conventional reactive strategies to assess differences in energy production,  
155 economic performance, and system reliability. This application demonstrates how adap-  
156 tive planning can inform long-term investment and operational decisions, enabling hy-  
157 dropower systems to sustain performance and resilience in an uncertain future.

158 Methodologically, HyTUNE advances hydropower adaptation by applying dynamic  
159 planning. Traditional robust planning seeks a single design that performs acceptably across  
160 many futures. In contrast, dynamic planning develops a policy that updates recursive  
161 decisions over time as new information emerges. This structure allows replacement path-  
162 ways to diverge as hydroclimatic trajectories unfold, so that planning decisions under  
163 progressively wetter futures can differ from those under drier futures, reducing regret un-  
164 der deep uncertainty (Herman et al., 2020). Dynamic planning frameworks have been  
165 successfully applied to a variety of water-resource management problems. Examples in-  
166 clude reservoir planning (S. Fletcher et al., 2019) and operation (Pei et al., 2024), ur-  
167 ban water-supply infrastructure adaptation (S. M. Fletcher et al., 2017; Zaniolo et al.,  
168 2023), and flood-risk management (Kwakkel et al., 2016) and planning (Hui et al., 2018).  
169 These approaches show how adaptive policies can adjust infrastructure and operational  
170 decisions in response to observed changes. While dynamic planning has been widely ex-  
171 plored in other water-management domains, it has not yet been applied to hydropower  
172 turbine planning and retrofitting.

173 The remainder of this study is organized as follows. Section 2 outlines the method-  
174 ological framework, including the development of the hydraulic model, reservoir oper-  
175 ation model, and retrofitting decision policy. Section 3 presents the case study, describ-  
176 ing plant characteristics and operational policies. Section 4 presents the performance anal-  
177 ysis of the proposed approach at the Hoover Hydropower Plant. Section 5 discusses the  
178 study’s limitations and outlines directions for future work. Finally, Section 6 provides  
179 an overview of the U.S. hydropower fleet and summarizes the key findings and highlights  
180 the broader implications for hydropower modernization and climate adaptation.

## 181 **2 Methodology**

182 The proposed decision-support framework integrates a tightly coupled suite of mod-  
183 els into a single modeling framework (Figure 1). The first component is a physics-based  
184 hydraulic simulator which computes power output at the Hydropower Plant (HP) as a  
185 function of reservoir release, level, and turbine configuration. The simulator considers  
186 variable turbine-efficiency curves and accounts for turbine specifications, frictional losses,  
187 minor losses, and dynamic tailwater elevations. The hydraulic simulator is nested within  
188 a reservoir operations model calibrated to historical records, which takes inflow and de-  
189 mand as inputs and produces time series of storage and releases. The final component  
190 is a dynamic planning optimization module that embeds the hydraulic and reservoir sim-  
191 ulators. It uses hydrological conditions as inputs and outputs decisions such as turbine  
192 replacement schedules, head adjustments, and discharge modulation. In this framework,  
193 the hydraulic and hydrological models are calibrated to the case study, while the dynamic  
194 planning module is optimized to maximize net present value (NPV) under uncertainty.

### 196 **2.1 Hydraulic model development**

197 Hydraulic models are fundamental to accurately capture efficiency fluctuation in  
198 reservoir-based HP. Specifically, physics-based hydraulic models track the movement of  
199 water from reservoir intakes through penstocks to turbine runners, resolving time-varying  
200 frictional and minor head losses and capturing turbine efficiency as a function of reser-  
201 voir head, release, and tailwater elevation. Modeling efficiency fluctuations in detail is  
202 necessary to enable the accurate calculation of dynamic HP power output.

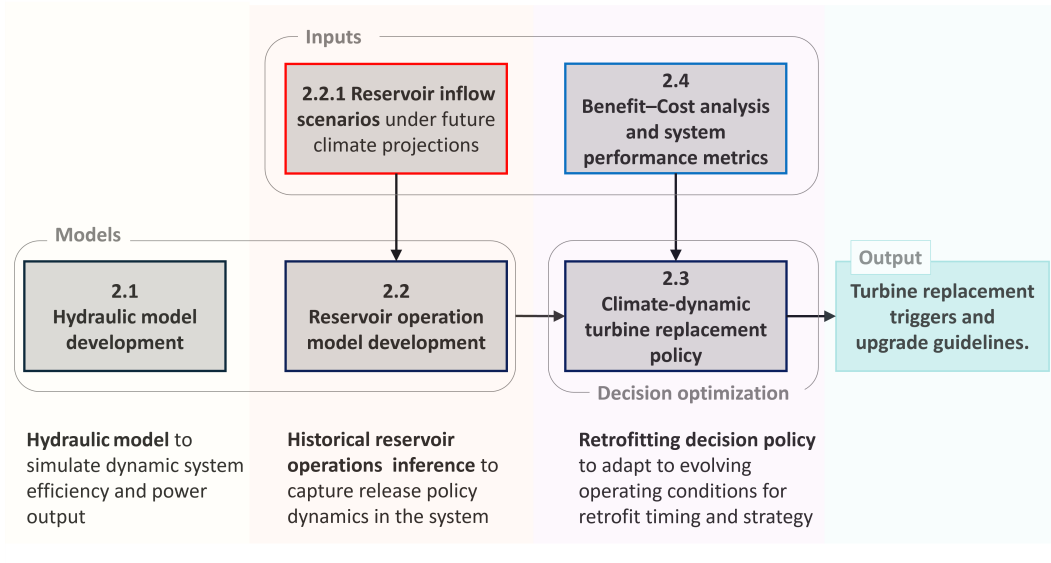


Figure 1: Methodological flowchart for our decision-support framework, with each step linked to the corresponding sections of the paper for detailed discussion.

203 The simulated daily HP generation,  $E_{sim}$ , (in kWh) for day  $t$  can be calculated as:

$$204 \quad E_{sim}(t) = \rho g H(t) Q(t) \eta(t) 24 \quad (1)$$

205 where  $\rho$  denotes the volumetric mass density of water ( $\text{kg}/\text{m}^3$ ),  $g$  is the gravitational ac-  
 206 celeration constant ( $\text{m}/\text{s}^2$ ),  $H(t)$  is the net hydraulic head (m),  $Q(t)$  is the volumetric  
 207 water flow rate ( $\text{m}^3/\text{s}$ ), and  $\eta(t)$  is the turbine efficiency (dimensionless). Note that both  
 208  $H$  and  $\eta$  are time dependent and vary based on turbine inflow, penstock diameter and/or  
 209 design flow, respectively. The simulated energy output,  $E_{sim}$ , also accounts for turbine  
 210 outage probability as a function of age, as described in the Supplementary Information.

211  $H(t)$  is calculated as the dynamic difference between reservoir level and tailwater  
 212 elevation (i.e., the level of the downstream river or water body that water is discharged  
 213 into) adjusted for frictional and minor losses, namely:

$$H(t) = H_{REL}(t) - H_{TEL}(Q, t) - H_f(Q, t) - H_o(Q, t) \quad (2)$$

214 where  $H_{REL}(t)$  is the reservoir water level and  $H_{TEL}(Q, t)$  is the downstream water level  
 215 at the tailrace, their difference is often referred to as the gross head. The friction losses  
 216 in the penstock and tunnel (if present) are denoted as  $H_f(Q, t)$ , while  $H_o(Q, t)$  accounts

217 for the total hydraulic (local) losses within the conveyance system. All heads and losses  
 218 are expressed in meters.

219 Tailwater elevation  $H_{\text{TEL}}(Q, t)$  is a function of the reservoir release and is usually  
 220 calculated based on historical measurements or HP design documents. Friction losses oc-  
 221 cur as water flows through penstocks or tunnels, increasing with flow velocity and pipe  
 222 roughness. Minor (or local) hydraulic losses arise from turbulence at bends, valves, and  
 223 transitions within the conveyance structure, and also scale with velocity and structural  
 224 design. Equation 3 details these losses as a function of plant physical properties and flow.  
 225 It consists of three key elements: the first term sums the friction losses in the  $Z$  series-  
 226 connected pipes via the Darcy–Weisbach equation, the second term accounts for tunnel  
 227 friction losses (if present) using the Manning formula; and the third term captures lo-  
 228 cal (minor) losses in those same  $Z$  pipes.

$$H_f(Q, t) = \sum_{\chi=1}^Z \left[ f_{\chi}(\epsilon, t) \frac{L_{\chi}}{D_{\chi}} \frac{V_{\chi}(t)^2}{2g} \right] + L_{\tau} \left( \frac{nV_{\tau}(t)^2}{R^{2/3}} \right)^2, \quad H_o(Q, t) = \sum_{\chi=1}^Z \left[ K_{\chi} \frac{V_{\chi}(t)^2}{2g} \right], \quad (3)$$

$$V_i(t) = \frac{Q_i(t)}{A_i}, \quad i \in \{\chi, \tau\}.$$

229 where  $V_{\chi}$  (m/s) represents the flow velocity in the  $\chi$ th pipe,  $f$  is a dimensionless  
 230 friction factor (function of pipe roughness  $\epsilon$ ),  $L_{\chi}$  (m) is the length of the  $\chi$ th pipe,  $D_{\chi}$   
 231 (m) denotes the diameter of the  $\chi$ th pipe,  $g$  (m/s<sup>2</sup>) signifies gravitational acceleration,  
 232  $n$  is the Manning roughness coefficient,  $K_{\chi}$  (–) accounts for aggregate resistance factors  
 233 (intake trash racks, bends, transitions) in the  $\chi$ th pipe,  $V_{\tau}$  (m/s) represents the flow ve-  
 234 locity in the tunnel,  $L_{\tau}$  (m) is the length of the tunnel,  $R$  (m) corresponds to the hy-  
 235 draulic radius, and  $A$  (m<sup>2</sup>) is the cross-sectional area of the pipe or tunnel.

236 We note that in most water resources studies,  $H$  is usually approximated by reser-  
 237 voir level, but this approximation leads to overestimation of HP output especially when  
 238 operating them outside of their design conditions. Similarly, the efficiency  $\eta$  in Eq. 1 is  
 239 a function of turbine age, head ( $H$ ), and discharge ( $Q$ ). New turbines operating near their  
 240 design head and discharge typically achieve efficiencies of about 90 %, but performance  
 241 declines sharply outside these ranges. Many water-resources studies simplify by assum-  
 242 ing a constant efficiency of 90 %, which systematically overestimates hydropower pro-  
 243 duction outside of design ranges (Fälth et al., 2023). Research highlights measurable de-  
 244 clines in turbine efficiency over time. Documented studies report age related reductions

245 that can be expressed as approximate annual rates (e.g., Goldberg & Lier, 2011; Quar-  
 246 anta et al., 2021), which supports modeling turbine efficiency as a linear function of age  
 247 in this study:

$$\eta_j(t) = \eta_0(Q, H) [1 - \lambda \mu(t)], \quad \lambda = \frac{\omega}{L_s} \quad (4)$$

248 where  $\eta_0(Q, H)$  denotes the baseline turbine efficiency as a function of discharge and head,  
 249  $\mu(t)$  is the turbine’s age in years (which resets to zero upon replacement),  $L_s$  represents  
 250 the designed service life in years, and  $\omega$  is the total percentage efficiency loss accumu-  
 251 lated over  $L_s$ . The relationship among discharge, head, and efficiency is illustrated in  
 252 the “hill” diagram in Figure ?? (SI). A typical Francis turbine (e.g. for moderate to large  
 253 head facilities) maintains high efficiency between 75 % and 120 % of its design head (ex-  
 254 pressed as the ratio of actual head to design head) and remains efficient down to about  
 255 50 % of its design flow.

256 After establishing the physical equations that govern the calculation of  $H$  and  $\eta$ ,  
 257 and therefore the energy production in a HP system, we calibrate the parameters that  
 258 appear in these equations based on historical observations of energy production, reser-  
 259 voir release, and reservoir level in our plant of interest.

260 We use a mixed literature-informed and data-driven approach. Literature allows  
 261 us to identify plausible ranges of these parameters for a HP, and within these ranges we  
 262 use a calibration approach to find the parameter combination that best explains the his-  
 263 torical relationship between  $E_{\text{sim}}$ ,  $Q$  and  $H$  in our plant of interest. Table ??, in SI, out-  
 264 lines recommended sampling ranges for the key hydraulic calibration parameters: pipe  
 265 roughness ( $\epsilon$ ), the Manning coefficient ( $n$ ), and the aggregate resistance factor ( $K$ ). Specif-  
 266 ically,  $\epsilon$  is varied between 0.03 mm and 2 mm,  $n$  between 0.011 and 0.018, and  $K$  be-  
 267 tween 0.5 and 5. These ranges reflect the broad variability introduced by factors such  
 268 as the age and internal surface condition of conduits, the geometric attributes of bends  
 269 and transition structures, and the flow distribution at elbows (Wahl & Cohen, 1999). We  
 270 also account for turbine efficiency degradation ( $\omega$ ) over the service life. Industry assess-  
 271 ments report efficiency losses of up to 8 % over 30 years (Quaranta & Hunt, 2022). Ac-  
 272 cordingly, we extend this range to 10–15 % to represent a service life of approximately  
 273 60 years. Using these parameter ranges, we run the hydraulic model hundreds of thou-  
 274 sands of times with a search algorithm, iterating until the simulated energy production  
 275 closely matches observed data. The fit is optimized by minimizing an objective function,

276 such as the mean absolute error, as described in Equation 5, ensuring accurate alignment  
 277 with real-world conditions.

$$\min_{\epsilon, n, K, \omega} J = \frac{1}{N} \sum_{i=1}^N \left| E_{\text{actual},i} - E_{\text{sim},i}(\epsilon_\chi, n, K_\chi, \omega) \right| \quad (5)$$

278 where  $E_{\text{actual},i}$  denotes the observed energy output for the  $i$ th observation, and  $E_{\text{sim},i}(\epsilon_\chi, n, K_\chi, \omega)$   
 279 represents the simulated energy output based on the hydraulic loss parameters  $\epsilon_\chi$ ,  $n$ ,  $K_\chi$   
 280 and  $\omega$ . Here,  $N$  signifies the total number of observations. It is important to note that  
 281 penstock's surface roughness,  $\epsilon_\chi$ , is related to the penstock friction factor,  $f_\chi$ ; therefore,  
 282 optimizing  $\epsilon_\chi$  corresponds to adjusting the  $f_\chi$ .

## 283 **2.2 Reservoir operation model development**

284 The hydraulic model described above is nested within a reservoir operation model  
 285 that simulates reservoir level and releases based on inflow time series and an operating  
 286 policy. The reservoir water balance is expressed as:

$$S(t+1) = S(t) + [I(t) - Ep(t) - R(t)]\Delta t \quad (6)$$

287 where  $S(t)$  is the reservoir storage ( $\text{m}^3$ ) at time  $t$ ,  $I(t)$  is the inflow ( $\text{m}^3/\text{s}$ ),  $R(t)$   
 288 is the outflow ( $\text{m}^3/\text{s}$ ),  $Ep(t)$  represents evaporation losses ( $\text{m}^3/\text{s}$ ), and  $\Delta t$  is the model  
 289 time step (s). The outflow of dam-regulated reservoirs is determined by reservoir oper-  
 290 ators, who release water according to a set of rules, known as the "operating policy", that  
 291 determine how much water should be released based on inputs such as season, reservoir  
 292 storage, water and power demand, and recent inflows (Loucks & Van Beek, 2017; X. Liu  
 293 et al., 2011; Zhou & Guo, 2013). Accurately representing these policies is essential to sim-  
 294 ulate plant-specific reservoir dynamics and hydropower production over time.

295 The following two sections describe how we obtained simulations of reservoir in-  
 296 flows time series extending to 2100, and controlled outflows for Hoover HP to simulate  
 297 reservoir dynamics. This provides the dynamic boundary conditions for simulating tur-  
 298 bine discharge and head.

### 2.2.1 *Reservoir inflow scenarios*

299  
300 Regulated reservoir inflow scenarios of Hoover Dam are leveraged from the Third  
301 Secure Water Act Assessment on the impact of Climate Change on Federal Hydropower  
302 (Broman & Voisin, 2025; Kao et al., 2022). This dataset presents a suite of high-resolution  
303 downscaled hydro-climate projections over the conterminous United States (CONUS),  
304 based on selected global climate models (GCMs) from the Coupled Model Intercompar-  
305 ison Project Phase 6 (CMIP6). The GCM outputs are downscaled using either statis-  
306 tical (DBCCA) or dynamical (RegCM) approaches, with bias correction based on two  
307 meteorological reference datasets (Daymet and Livneh) (Kao et al., 2022a).

308 The downscaled precipitation, temperature, and wind speed are used to drive two  
309 calibrated hydrologic models, VIC and PRMS, enabling the simulation of projected hy-  
310 drologic responses across CONUS (Naz et al., 2016; Kao et al., 2022). This process pro-  
311 duces an ensemble of 56 daily runoff projections spanning 1981–2099 under multiple emis-  
312 sion scenarios. The runoff projections are then routed through the mosartwmpy water  
313 management and river routing framework (Voisin et al., 2013; Thurber et al., 2021), which  
314 simulates regulated streamflow, including reservoir operations based on historically de-  
315 rived policies (Turner et al., 2022; Broman et al., 2024) and accounting for sectoral wa-  
316 ter withdrawals (Voisin et al., 2017). The resulting dataset provides reservoir inflows that  
317 serve as inputs to our reservoir operation model, described in the next session.

### 318 2.2.2 *Historical reservoir operations (HRO) inference*

319 In dam-controlled reservoirs, releases are determined through an "operating pol-  
320 icy" as a function of season, reservoir storage, water and power demand (Loucks & Van Beek,  
321 2017; X. Liu et al., 2011; Zhou & Guo, 2013). Accurately representing these policies is  
322 essential to simulate plant-specific reservoir dynamics and hydropower production over  
323 time. In some cases, documented rule curves or operational guidelines are available in  
324 dam documentation or regulatory filings, but such information is not always accessible  
325 or up to date. In cases where formal operating rules are unavailable, release behavior can  
326 be inferred directly from historical inflow, storage, and outflow records using machine-  
327 learning techniques (Fakhfakh et al., 2017).

328 In recent years, deep learning methods such as long short-term memory (LSTM)  
329 networks have gained popularity in reservoir operation modeling, particularly for pre-

330 dicting water releases (Zhang et al., 2019; Wang et al., 2022). LSTMs effectively cap-  
 331 ture complex temporal patterns and nonlinear dynamics in hydrologic systems (Al-Hardanee  
 332 & Demirel, 2024; Feng et al., 2023; Barzola-Monteses et al., 2022), allowing them to ap-  
 333 proximate the nuanced decision-making of experienced operators. In this study, we em-  
 334 ploy an LSTM network to model temporal dependencies in the reservoir operation time  
 335 series. The full model setup, input structure, model parameter tuning, and training pro-  
 336 cedure are provided in the Supplementary Information.

### 337 **2.3 Climate-dynamic turbine replacement policy**

338 Water resource systems are undergoing unprecedented changes in water supply  
 339 and demand that require planning strategies to adapt to evolving hydrologic conditions  
 340 (Herman et al., 2020). We formulate the turbine replacement problem as a control prob-  
 341 lem that suggests turbine replacement timing and configuration as a function of the sys-  
 342 tem state, such as observable reservoir levels averaged over different time windows and  
 343 system efficiency.

344 As illustrated in Panel A of Figure 2, the model begins by comparing a feature of  
 345 the system condition (e.g.,  $\text{Feature}_1$ , reservoir levels) to a threshold. If the condition is  
 346 met ("Yes"), the process proceeds to the next decision node (e.g., checking  $\text{Feature}_2$ , ef-  
 347 ficiency); otherwise, a default action (e.g., no replacement) is selected. Panel B of Fig-  
 348 ure 2 presents the optimized decision tree, which is detailed in the following sections.

349 The decision tree's structure, features, threshold values, and actions, are determined  
 350 through an evolutionary simulation–optimization algorithm that iterates over hundreds  
 351 of thousands of simulations for an ensemble of climate scenarios. The evolutionary al-  
 352 gorithm applies operators such as mutation, crossover, and selection, to identify the tree  
 353 configuration that maximizes net present revenue, calculated as the expected difference  
 354 between energy revenue and turbine replacement costs. The optimized decision tree de-  
 355 termines when to schedule turbine replacements and how to adjust their configuration  
 356 (such as head and capacity) as a function of relevant system indicators such as reservoir  
 357 head and turbine age. This approach was developed in (Cohen & Herman, 2021) and sub-  
 358 sequently used in (Zaniolo et al., 2023) for a problem of urban water planning.

359 The following table summarizes the key decision actions and input features used  
 360 in the model. Panel A of Table 1 organizes the 82 possible actions into four categories:

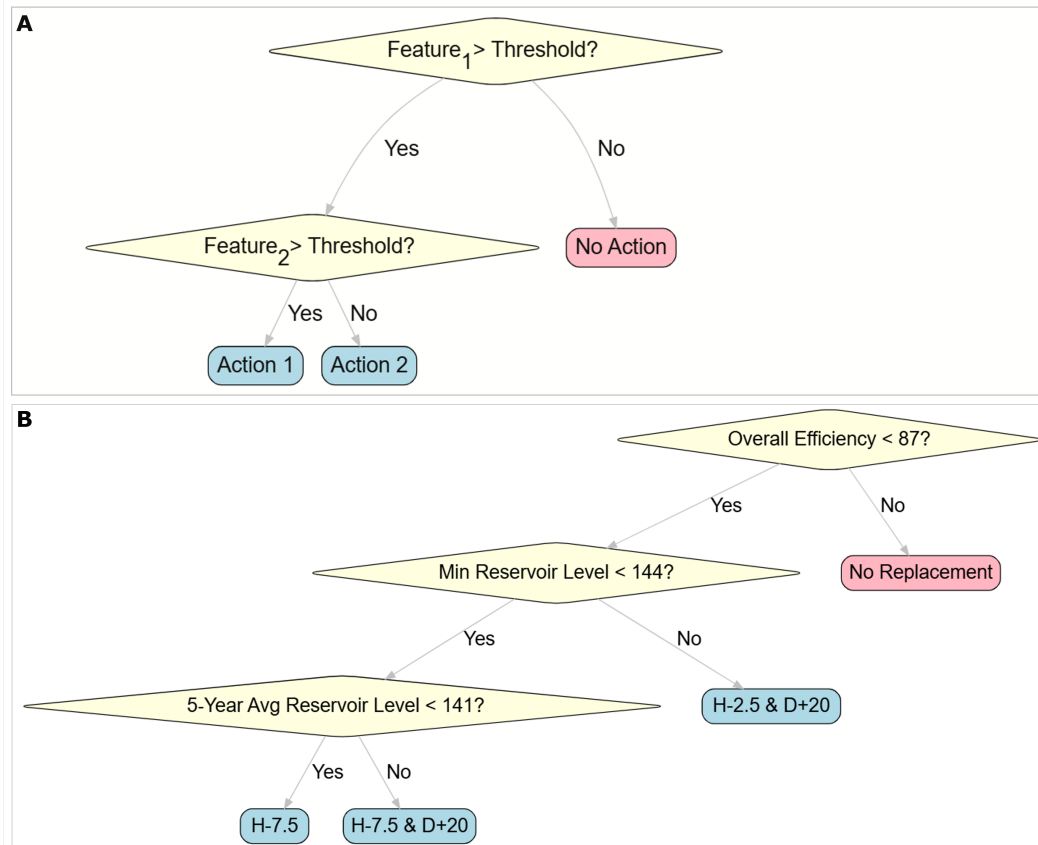


Figure 2: Panel A: Schematic of the decision tree model for hydropower planning. The model sequentially evaluates system features, beginning with a primary attribute (e.g., Feature<sub>1</sub>) compared to a threshold. A “Yes” may branch to further nodes (e.g., Feature<sub>2</sub>), while a “No” can terminate the path or trigger an action. Subsequent nodes similarly map system states to distinct operational actions. Panel B: Optimized decision tree showing the optimized structure.

361 no replacement, head adjustments, discharge adjustments, and combined adjustments.  
 362 Panel B lists the 11 input features that describe the state of the hydropower system and  
 363 inform the model’s decision rules.

#### 364 **2.4 Benefit–Cost analysis and system performance metrics**

365 Replacing hydropower turbines is a multimillion-dollar investment that shapes sys-  
 366 tem reliability and energy generation capacity for decades into the future. Choosing what  
 367 turbines to replace, when, and with what configuration (or conversely extending the life  
 368 of existing units through repair) requires a careful weighing of capital costs against the  
 369 benefits of higher conversion efficiency, greater operational flexibility, and improved re-

Table 1: Decision actions and model input features

<b>A) Grouped decision actions</b>	
<b>Category</b>	<b>Action options</b>
No/Replacement	No Replacement; Replace Existing
Head Adjustments	H+2.5, H+5, . . . , H-10
Discharge Adjustments	D+5, D+10, . . . , D-20
Combined H & D	All combinations (e.g. H+2.5 & D+5, . . . ) (See Table ?? (in SI) for the complete list of 82 actions)
<b>B) Input features</b>	
<b>Feature</b>	<b>Explanation</b>
5-Year Avg Reservoir Level	5-year average net reservoir head
10-Year Avg Reservoir Level	10-year average net reservoir head
Max Reservoir Level	5-year maximum reservoir level
Min Reservoir Level	5-year minimum reservoir level
5-Year Avg Reservoir Release	5-year average reservoir release for power production
10-Year Avg Reservoir Release	10-year average reservoir release for power production
Upper Nominal Head	Design head of higher-head turbines
Lower Nominal Head	Design head of smaller-head turbines
Overall Efficiency	Overall system efficiency
Peak Efficiency	Peak efficiency of new turbines over a five-year period
Minimum Efficiency	Minimum efficiency of old turbines over a five-year period

370 liability. In the next three sections we report how we quantify the costs of replacement  
371 and benefits measured as the net present value of incremental hydropower revenue. We  
372 also present several other performance metrics used to further assess our turbine replace-  
373 ment policies such as firm energy production and capacity factors.

#### 374 ***2.4.1 Benefits: hydropower revenue estimation***

375 Benefits of hydropower plants are derived from the projected revenue generated over  
376 the project’s operational lifetime, based on the expected energy production and the cor-  
377 responding electricity market prices. Since electricity prices fluctuate throughout the day,  
378 energy output must be estimated across distinct time-of-use segments, namely, peak, mid-  
379 day, and off-peak periods. Although the exact timing of these segments varies by region  
380 and season (FERC, 2024; EIA, 2025), we adopt a simplified (generalized) approach, based  
381 on commonly observed U.S. wholesale electricity market dynamics (FERC, 2024; Mill-  
382 stein et al., 2025), dividing the day into three pricing blocks: 6 hours for peak, 12 hours  
383 for mid-day, and 6 hours for off-peak.

384 The annual revenue  $AR_y$  (in USD) for year  $y$ , over a period of  $\Delta t$  days, is obtained  
 385 by summing the daily energy outputs in each tariff segment multiplied by their respec-  
 386 tive prices:

$$387 \quad AR_y = \sum_{t=1}^{\Delta t} \sum_{j=1}^K E_{\text{sim},j}(t) e_{p,j}, \quad K \in \{1, 2, 3\} \quad (7)$$

388  $K \in \{1, 2, 3\}$  indexes the three daily segments (peak, mid-day, and off-peak);  $E_{\text{sim},j}(t)$   
 389 (kWh) is the simulated energy in segment  $j$  on day  $t$ ; and  $e_{p,j}$  (USD/kWh) is the price  
 390 for that segment.

391 Next, the lifetime expected net present revenues from hydropower production can  
 392 be determined as follows:

$$393 \quad R = \sum_{y=1}^{L_s} \frac{AR_y}{(1 + r_y)^y} \quad (8)$$

394 where  $L_s$  denotes the project's lifetime. The vectors  $\mathbf{R} = \{R_1 \dots, R_{L_s}\}$  and  $\mathbf{r} = \{r_1, \dots, r_{L_s}\}$   
 395 represent the annual plant revenues (assuming average hydropower production through-  
 396 out the year, in USD) and the annual interest (discount) rates in percentage, respectively,  
 397 both over the project's lifetime.

398 HyTUNE is designed to adapt turbine replacement to nonstationary hydrology, but  
 399 here we do not evaluate how long-term changes in electricity prices could alter replace-  
 400 ment decisions. Credible projections of future prices require an explicit representation  
 401 of power-system evolution and market dynamics, which is beyond the scope of this ini-  
 402 tial methodological contribution. We therefore represent intra-day price variability, but  
 403 treat longer-term electricity price trajectories as exogenous and time-invariant.

#### 404 **2.4.2 Costs: hydropower turbine replacement**

405 We use the Baseline Cost Model (BCM) for hydropower projects developed by Oak  
 406 Ridge National Laboratory (Oladosu & Ma, 2025) to estimate retrofit costs. For projects  
 407 with added capacity greater than 30 MW and hydraulic head exceeding 60 ft, the cost  
 408 model is expressed as:

$$RC = \zeta \theta \exp \left[ \beta_0 + \beta_1 \ln(\text{AddedCap}) + \beta_2 \ln(\text{Head}) \right] \quad (9)$$

409 Turbine replacement costs ( $RCs$ ) are estimated as a nonlinear function of installed  
 410 capacity, design head, and categorical model terms. The full model expression, includ-  
 411 ing all parameters used in this study, is provided in the Supplementary Information. A  
 412 detailed description of the BCM and its components is available in O'Connor et al. (2015);  
 413 Oladosu and Ma (2025).

414 The lifetime expected net present cost of turbine replacement is then computed as

$$415 \quad C = \sum_{n=1}^N \frac{RC_n}{(1 + r_{T_n})^{T_n}} \quad (10)$$

416 where  $N$  is the number of replacement events and  $T_n$  is the year in which the  $n^{th}$  replace-  
 417 ment occurs.

### 418 **2.4.3 Performance metrics: NPV and other reliability metrics**

419 In this framework, design optimization relies on financial performance measures,  
 420 emphasizing the lifetime net present value of benefits and costs. The primary objective  
 421 is to maximize the net present value (NPV), which aggregates projected cash flows dis-  
 422 counted to the present (Santolin et al., 2011). The NPV is defined as:

$$423 \quad f_{NPV} = R - C \quad (11)$$

424 In this study, we use fixed energy prices of \$90/MWh (peak), \$50/MWh (mid-day),  
 425 and \$30/MWh (off-peak) to represent western market dynamics and price variability.  
 426 A 3 % discount rate was used, consistent with U.S. hydropower feasibility standards. De-  
 427 tailed assumptions and data sources are described in the Supplementary Information Sec-  
 428 tion ??.

429 While our policies are trained to maximize NPV, we also evaluate their performance  
 430 across several additional indicators that capture broader aspects of hydropower opera-  
 431 tion. We benchmark the optimized HyTUNE policy (OPT) against two reactive approaches  
 432 that reflect common industry practice. In the first approach ( $RA_1$ ), all turbines are re-  
 433 placed with identical units after 55 years of operation. In the second approach ( $RA_2$ ),  
 434 identical replacements occur twice, after 40 and 80 years of operation. For the perfor-  
 435 mance comparison, metrics with the subscript OPT refer to the HyTUNE strategy, and  
 436 metrics with the subscript RA refer to the reactive approaches:

$$\Delta AAE = AAE_{OPT} - AAE_{RA}$$

$$\Delta NPV = NPV_{OPT} - NPV_{RA}$$

$$FPG = E_{OPT, 0.05} - E_{RA, 0.05} \quad (12)$$

$$\Delta PP = 365 \times \mathbb{E}[E_{OPT, peak} - E_{RA, peak}]$$

$$EG_{IP} = \left[ \sum E_{OPT} / \sum OPT_{cap} \right] \div \left[ \sum E_{RA} / \sum RA_{cap} \right]$$

437 Here,  $\Delta AAE$  is the change in annual average energy generation (GWh),  $\Delta NPV$  is the  
 438 change in net present value (M \$), FPG is the firm power gain, defined as the energy avail-  
 439 able 95 % of the time (MWh/day),  $\Delta PP$  is the change in peak-period energy generation  
 440 (GWh/year), representing the amount of energy produced during 6 daily peak hours, and  
 441  $EG_{IP}$ , analogous to a capacity factor, represents energy generated per installed capac-  
 442 ity.

### 443 3 Case study and data

444 The Hoover Hydropower Plant, completed in 1936 on the Colorado River, oper-  
 445 ates seventeen Francis turbines, nine on the Arizona side and eight on the Nevada side,  
 446 along with two 2.4 MW Pelton station-service units. Together they provide a total name-  
 447 plate capacity of about 2,080 MW (USBR, 2018). Water enters the powerhouse through  
 448 four 9.15 m penstocks that divide into 3.97 m pipes feeding the main turbines.

449 Figure 3 shows monthly reservoir elevation and discharge at Hoover HP from 1938  
 450 to 2023. After 2000, reservoir levels declined sharply as drought persisted and regional  
 451 water demand increased. The drop in elevation reduced the gross head, defined as the  
 452 difference between reservoir level and tailwater, and lowered power generation capacity  
 453 (Hannoun & Tietjen, 2023; Huizar et al., 2024). Despite declining reservoir levels, the  
 454 data show that discharges (blue line) remained relatively stable with seasonal variabil-  
 455 ity.

456 Hoover's original HP design required a minimum power-pool elevation of 320 m.  
 457 From 1986 to 1993, operators upgraded all Francis turbines to higher-capacity versions  
 458 while maintaining the same design head (Rogers, 2010; M. Johnson et al., 2023). As Lake  
 459 Mead levels continued to fall, these uprated units lost efficiency. Between 2012 and 2015,

460 operators replaced five turbines with low-head models optimized for reduced water lev-  
 461 els (Farmer, 2020; M. Johnson et al., 2023). This is a rare example of a heterogeneous  
 462 turbine configuration retrofit that had the effect of lowering the minimum power-pool  
 463 to about 290 m thereby extending the plant’s operating range during continued storage  
 464 decline (Tweed, 2013; Jenkin et al., 2019).

465 Water management on the Colorado River requires balancing multiple and often  
 466 competing objectives. State agencies, Native American tribes, irrigation districts, mu-  
 467 nicipalities, and environmental groups depend on the river for municipal, agricultural,  
 468 industrial, recreational, and ecological needs (Abboud et al., 2022). High hydrologic vari-  
 469 ability adds further complexity (McCoy et al., 2022; Smith et al., 2022). The “Law of  
 470 the River,” a collection of compacts, treaties, and statutes, governs allocations, release  
 471 schedules, and storage priorities throughout the basin (Lukas & Payton, 2020; Wheeler  
 472 et al., 2022; Fleck & Castle, 2022). All water releases for both downstream delivery and  
 473 hydropower generation must follow these rules (see Table ?? in the Supplementary In-  
 474 formation). As a result, operational decisions account not only on reservoir levels and  
 turbine efficiency but also on legal allocations and environmental mandates.

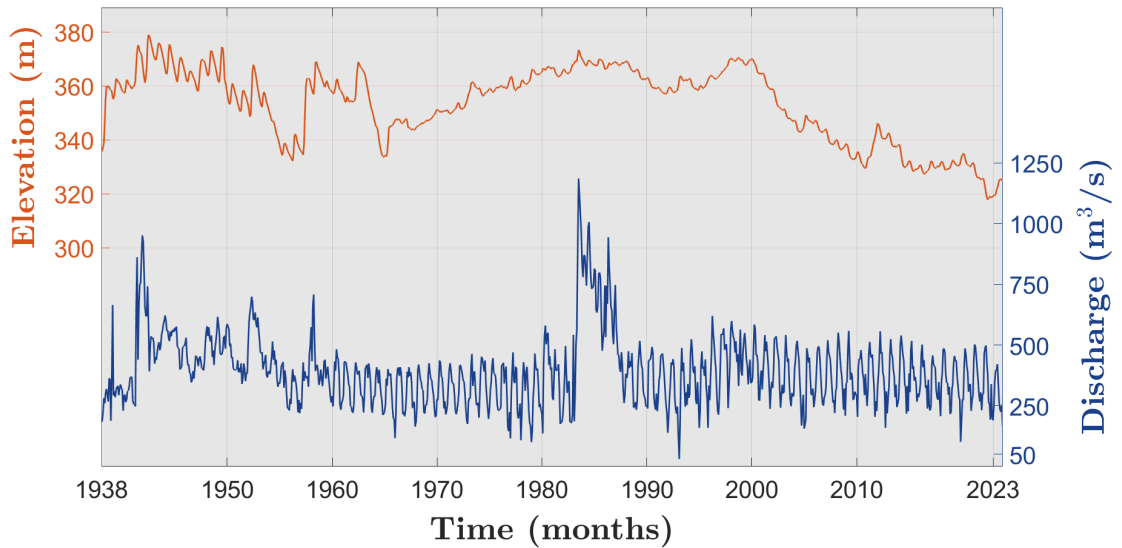


Figure 3: Temporal evolution of Hoover Dam reservoir elevation and discharge. The left y-axis (orange) indicates reservoir elevation (m), and the right y-axis shows discharge ( $\text{m}^3/\text{s}$ ). The data represent monthly averages, with the x-axis denoting time in months.

475

## 4 Results

### 4.1 Hydraulic model calibration

We calibrated the hydraulic model using operational and hydrological data following the setup described in Section 2.1. Here, calibration means identifying the uncertain parameters in the physical loss and performance equations, such as penstock roughness and local loss coefficients, that allow simulated daily generation to match observed plant output under observed forcing. We used daily inflow and energy-generation records available from 1980 onward, and calibrated over 1980–2023. We compute tailwater elevation as a function of downstream conditions, using elevation observations at Davis Dam, located 108 km downstream and forming Lake Mohave. When the water level at Davis Dam exceeds 195 m (638 ft), tailwater at Hoover rises. We use this relationship to estimate tailwater elevation at the plant and compute gross head as the difference between reservoir elevation and tailwater level. Net head then follows from Eq. 2 after accounting for friction and local losses.

We performed calibration with a Monte Carlo search. We generated  $M = 10,000$  parameter sets within the literature-informed ranges reported in SI Table ???. The calibrated parameters include penstock roughness ( $\epsilon$ ), local loss coefficients ( $K_1$ ,  $K_2$ ), and turbine efficiency degradation ( $\omega$ ). For each parameter set, we simulated the full calibration period and computed the objective function  $J$  in Eq. 5, defined as the mean absolute error between simulated and observed daily generation. The best-fitting parameter set defines the calibrated model, which we then force with future inflow projections to translate hydrologic change into projections of hydropower generation.

Panel A of Figure 4 shows the Monte Carlo search space of  $(K_1, K_2, \epsilon)$ , where marker color indicates  $J$  and size represents  $\omega$ . The optimal parameter set is  $\epsilon = 0.636$  mm,  $K_1 = 0.605$ ,  $K_2 = 0.553$ , and  $\omega = 8.87\%$ , yielding  $J = 0.512$ . Panel B presents a two-dimensional cross-section at  $\epsilon = 0.636$  mm. When both  $K_1$  and  $K_2$  exceed 2, variations in  $\omega$  produce only minor changes in  $J$ . This pattern shows that hydraulic head-loss parameters dominate the calibration, while efficiency degradation plays a secondary role. Panel C compares observed and simulated power generation aggregated to monthly averages for clarity, with the daily comparison provided in the Supplementary Information (Figure ??). The black line shows observed generation, and the gold line shows modeled output from the calibrated parameter set. The two curves align closely in both am-

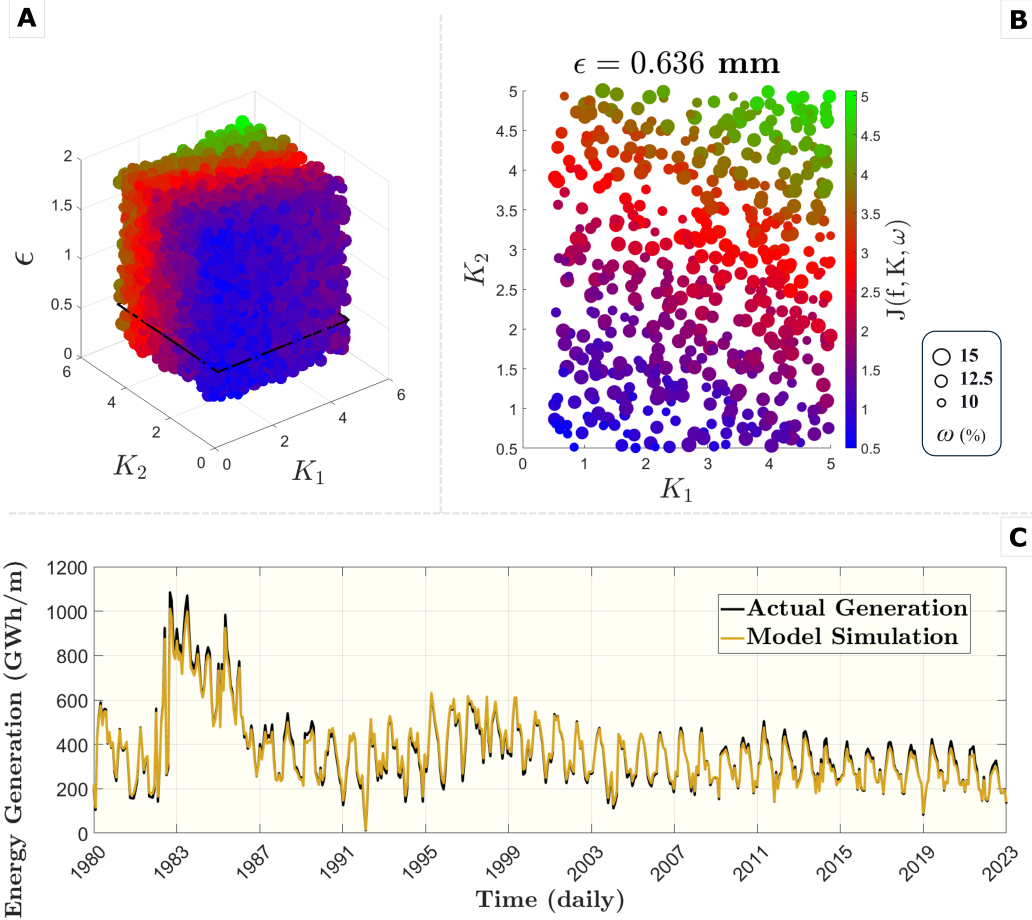


Figure 4: **Panel A:** 3D scatter plot of Monte Carlo-sampled parameter sets  $(K_1, K_2, \epsilon, \omega)$ , where marker color encodes the objective function  $J$  and marker size encodes turbine efficiency loss  $\omega$  (legend at right: smallest circles = 10%, largest circles = 15% after 60 years of operation). **Panel B:** 2D cross-section at  $\epsilon = 0.636$  mm, illustrating the sensitivity of  $J$  to variations in the minor-loss coefficients  $K_1$  and  $K_2$  and efficiency loss  $\omega$ , using the same color and size mappings as in the left panel. **Panel C:** Monthly-aggregated power production (GW) at Hoover HP: observed generation (black line) versus simulated output (golden line) from the calibrated hydraulic model using the optimized parameter set and historical inflow records. Daily data (1980–2023) were averaged to monthly resolution.

508 plitude and timing, reproducing seasonal and interannual variations with high fidelity.  
 509 This agreement demonstrates that the calibrated model captures Hoover’s operational  
 510 behavior and provides a reliable basis for assessing future performance under climate-  
 511 driven inflow scenarios.

## 4.2 Historical Reservoir Operation inference

After completing the model selection process described in Section 2.2.2, we apply the calibrated LSTM architecture to predict reservoir releases under a wide range of future climate scenarios.

Figure 5 summarizes the model trajectories linking projected inflows, model performance, and reservoir response under future climate scenarios. Panel A shows historical inflows (1938–2023; weekly data, 10-year moving average; gray) and bias-corrected CMIP6 inflow projections (purple). The darker purple line represents the multi-scenario mean. The historical record declines through the 1970s, then rises into the 1990s. The 10-year smoothing highlights long-term variability rather than short-term fluctuations. Projected inflows show a broader spread by mid and late century, reflecting increasing hydrologic uncertainty across the CMIP6 ensemble. Panel B evaluates the performance of the LSTM reservoir operation model. Observed discharge (solid gray) and model predictions (dashed red) align closely across the training and validation periods, with the shaded region marking the validation window. The model achieves  $R^2 = 0.83$  during training and  $R^2 = 0.67$  during validation, demonstrating its ability to capture nonlinear relationships among inflow, storage, and release. Panel C outlines the modeling workflow, where bias-corrected inflow projections drive the trained LSTM model to generate time-series estimates of discharge and reservoir elevation for each climate scenario. Panels D and E show the simulated reservoir releases and elevations, respectively. In Panel D, observed releases (gray) and modeled releases under future inflow scenarios (blue) share similar variability, with the darker blue line showing the ensemble mean. Panel E presents corresponding reservoir elevation trajectories (gold), with the darker line representing the mean across scenarios. Both panels show widening spreads after mid-century, indicating that inflow uncertainty propagates into increasingly variable operational outcomes. Some scenarios project persistently low reservoir levels, signaling risks to storage reliability and hydropower generation under drier futures. Overall, these results show that a data-driven reservoir model coupled with CMIP6 inflow projections can translate hydrologic uncertainty into plausible ranges of future discharge and storage.

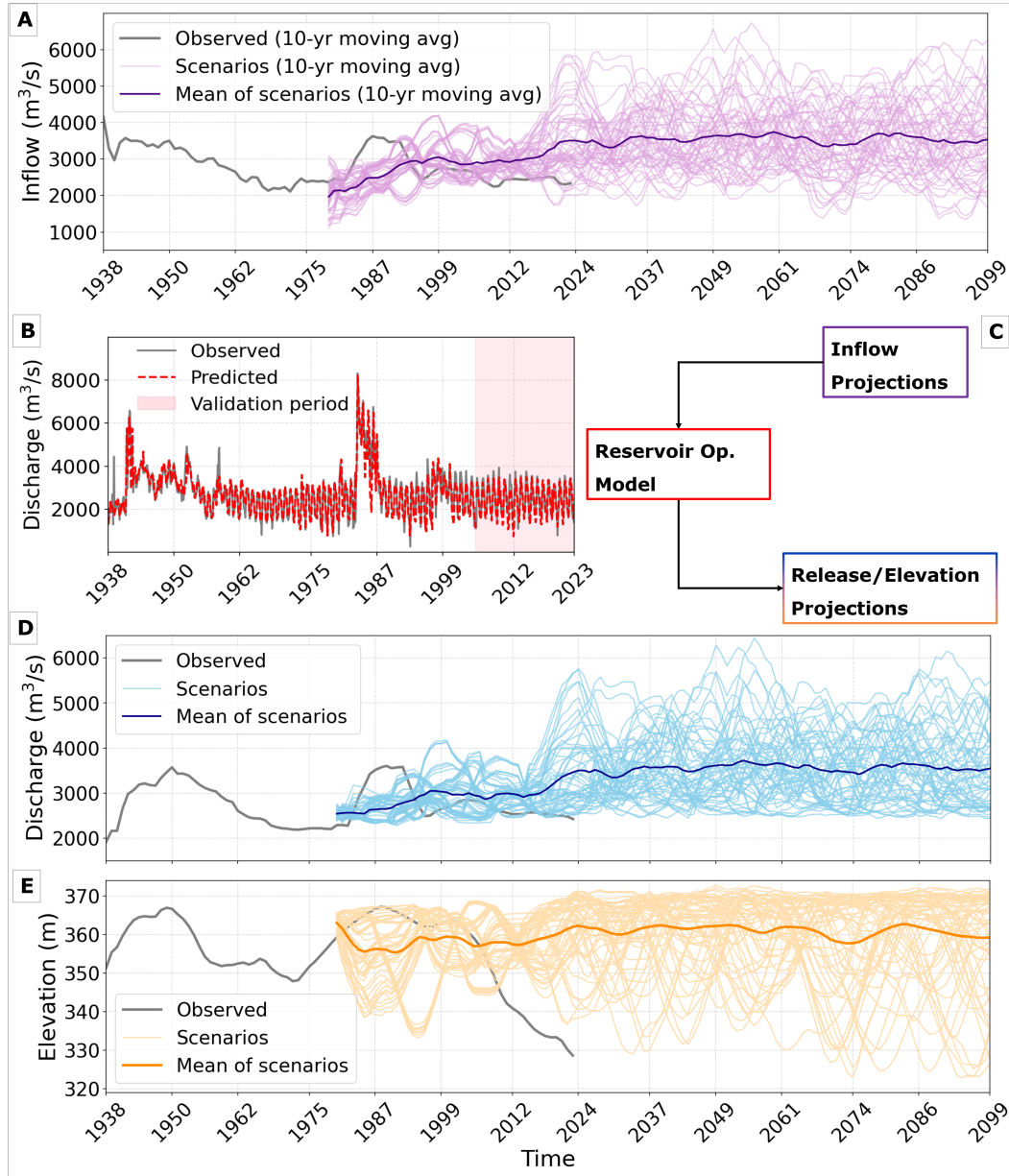


Figure 5: Observed and projected inflows, model performance, and scenario-based reservoir simulations. (A) Historical inflow (gray) and bias-corrected CMIP6 projections (purple). (B) Observed and LSTM-predicted discharge with  $R^2$  of 0.84 and 0.67 for training and validation periods respectively. (C) Modeling workflow linking inflow projections to reservoir operation. (D–E) Simulated releases (blue) and elevations (gold) under future inflow scenarios, with darker lines denoting ensemble means. Results show divergent operational outcomes and potential low-storage futures under dry scenarios.

541

### 4.3 Climate dynamic turbine replacement policy

542

After simulating future releases and reservoir elevations, we performed a policy-

543

search optimization to optimize the structure and elements of the decision tree that spec-

544 ifies the replacement policy, effectively identifying under what conditions changing tur-  
545 bine head or capacity improves system performance, and to what designs with the ob-  
546 jective of maximizing NPV.

#### 547 **4.3.1 *Optimized policy tree***

548 HyTUNE uses policy search to develop a decision tree that defines optimal turbine  
549 replacement rules. The tree was trained on 80 % of randomly selected scenarios and tested  
550 on the remaining 20 %. The initial year of operation was set to 1985, the point at which  
551 climate scenario data become available and all turbines share the same design head. To  
552 evaluate performance, we benchmark the optimized HyTUNE policy (OPT) against two  
553 reactive approaches that follow fixed service life thresholds and do not account for sys-  
554 tem performance or changing conditions. In the first approach (RA<sub>1</sub>), all turbines are  
555 replaced with identical units after 55 years. In the second approach (RA<sub>2</sub>), identical re-  
556 placements occur twice, after 40 and 80 years of operation.

557 The resulting OPT of HyTUNE is shown in Figure 2. We confirmed the stability  
558 of through multiple optimization runs. Each optimization involved 250,000 function eval-  
559 uations and was repeated over 10 times (using 10 random seeds per run) to assess con-  
560 vergence consistency. Further details on the experimental setup are provided in the Sup-  
561 plementary Information. HyTUNE triggers a turbine replacement when the overall ef-  
562 ficiency of turbines drops below 87 %. When efficiency is higher, no replacement occurs.  
563 When efficiency falls below this threshold, the policy evaluates recent hydrologic states.  
564 If the 5-year minimum reservoir level is above 144 m, the framework recommends low-  
565 ering the design head by 2.5 % and increasing discharge capacity by 20 %. If the 5-year  
566 minimum level falls below 144 m, the model checks the 5-year average reservoir level. When  
567 this value is above 141 m, the framework increases discharge capacity by 20 % and de-  
568 creases head by 7.5 % . Otherwise, it lowers the design head by 7.5 %. This policy tree  
569 defines adaptive retrofit rules that balance hydraulic efficiency, energy output, and op-  
570 erational flexibility across a range of future hydrologic conditions.

#### 571 **4.3.2 *HyTUNE retrofitting adaptation to wet and dry futures***

572 To explore how HyTUNE is able to observe and dynamically adapt to changing con-  
573 ditions in the system, we simulate the optimized decision tree for the scenario with the  
574 lowest median reservoir level (dry scenario) and the one with the highest median reser-

575

voir level (wet scenario). Figure 6 illustrates reservoir dynamics and turbine replacement outcomes under these contrasting futures. The top panel shows projected reservoir el-

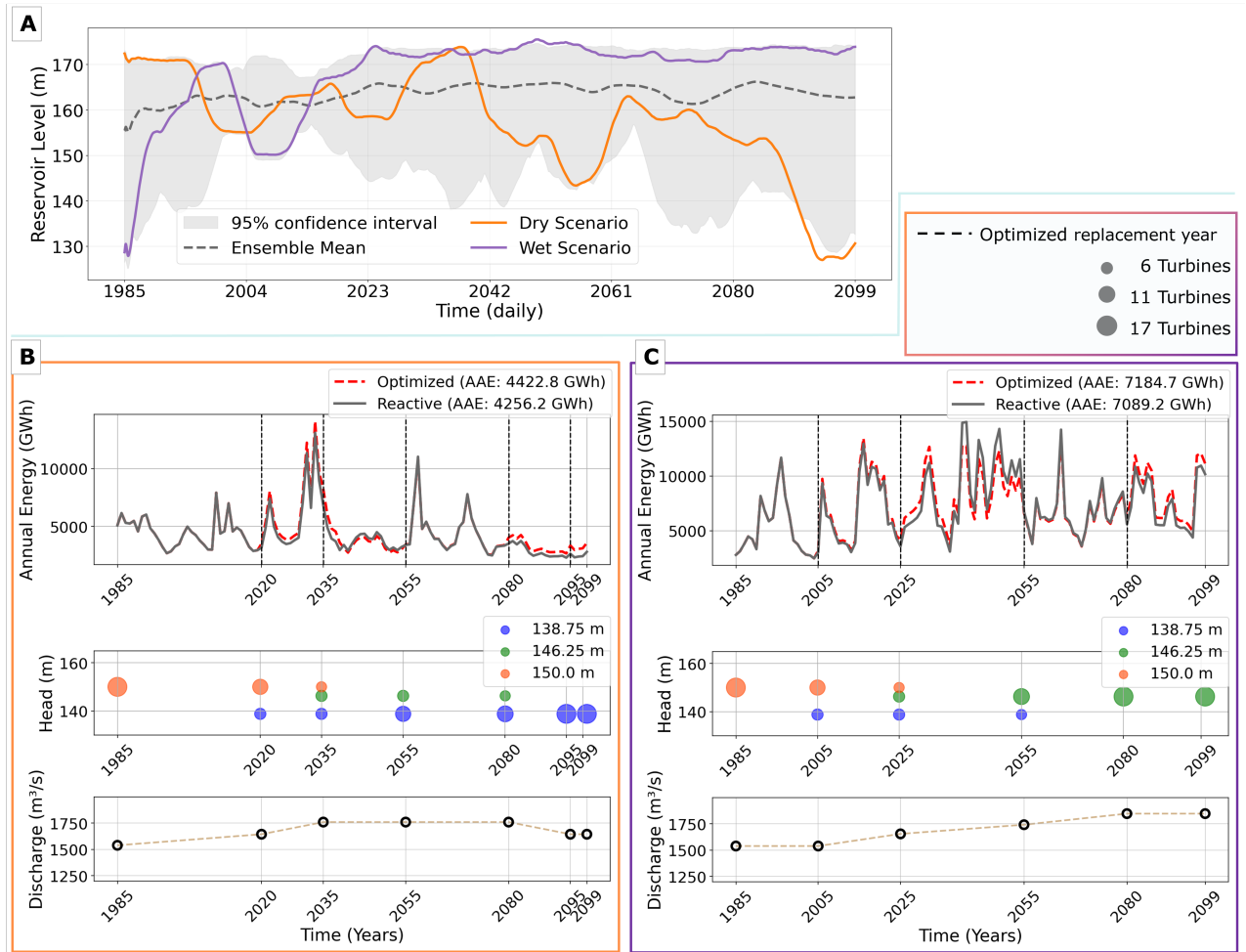


Figure 6: Reservoir dynamics and turbine replacement outcomes under diverse inflow scenarios. **Panel A:** Reservoir elevation trajectories for all projected inflow scenarios. The shaded gray region represents the 95 % confidence interval, and the dashed gray line shows the ensemble mean. The orange line marks the scenario with the lowest median reservoir level (dry scenario), while the purple line corresponds to the highest median reservoir level (wet scenario). **Panels B–C:** Effects of turbine replacement strategies on hydropower generation under the selected dry (left) and wet (right) scenarios. Each bottom panel includes three aligned plots: (i) annual energy generation (GWh) for the reactive one-time replacement strategy (solid gray) and the optimized replacement strategy (dashed red), with vertical dashed lines marking replacement years (black for optimized, blue for reactive); (ii) evolution of turbine design head over time, where circle size denotes the number of turbines operating at that head; and (iii) evolution of total design discharge over time. A separate legend in the top-right corner identifies the reactive and optimized replacement strategies for Panels B–C.

576

577

evaluations for all inflow scenarios. The shaded gray region marks the 95 % confidence in-

578 terval, and the dashed gray line indicates the ensemble mean, with the dry scenario shown  
 579 in orange and the wet scenario in purple. The bottom panels show the performance and  
 580 evolution of Hoover HP under these two representative scenarios using the optimized pol-  
 581 icy of HyTUNE. Each panel includes three time-aligned subplots. The top subplot presents  
 582 annual energy generation in GWh for the reactive one-time replacement strategy (RA<sub>1</sub>,  
 583 solid gray) and the OPT (dashed red). The middle subplot shows the evolution of tur-  
 584 bine design head, where symbol size represents the number of turbines operating at each  
 585 head. The bottom subplot depicts the evolution of total design discharge. In both the  
 586 dry and wet scenarios, the reactive approach replaces all 17 turbines simultaneously af-  
 587 ter 55 years of operation (blue dashed line).

588 Under the dry scenario (Panel B), the optimized policy (OPT) schedules five re-  
 589 placement phases involving a total of 29 turbines over several decades, resulting in higher  
 590 average annual energy (AAE = 4422.8 GWh) compared with the reactive approach RA<sub>1</sub>  
 591 (4256.2 GWh). Head variability reflects both hydrologic forcing and adaptive replace-  
 592 ment decisions. OPT first reduces the design head by 7.5 % (from the original 150 m)  
 593 and increases discharge by 20 % in 2020 by replacing six turbines. In 2035, it lowers the  
 594 design head by 2.5 % and again increases discharge by 20 % for another six turbines.  
 595 A third phase occurs in 2055, when OPT reduces design head by 7.5 % and increases dis-  
 596 charge by 20 % for the remaining five turbines, completing replacements across the 17-  
 597 unit fleet. By 2080, the system undergoes another partial replacement as efficiency drops  
 598 below the threshold, with six turbines replaced. This is followed by an additional six re-  
 599 placements in 2099, during which discharge is reduced to account for lower projected in-  
 600 flows. This phased strategy enables the plant to respond gradually to hydrologic change  
 601 while preserving operational flexibility for future adaptation.

602 In the wet scenario, the optimized policy (OPT) still yields higher long-term ben-  
 603 efits, with average annual energy (AAE = 7184.7 GWh) compared with 7089.2 GWh for  
 604 RA<sub>1</sub>. OPT follows a distinct pattern of phased replacements. In 2005, it reduces design  
 605 head by 7.5 % for six turbines. In 2025, it lowers head by 2.5 % and increases discharge  
 606 by 20 % for another six turbines. A third phase in 2055 applies the same 2.5 % head re-  
 607 duction and 20 % discharge increase to the remaining five turbines. By 2080, higher reser-  
 608 voir levels allow the framework to restore the first six low-head turbines to a head of 138.75  
 609 m (2.5 % below the original) while maintaining a 20 % increase in discharge capacity.  
 610 Across both scenarios, the optimized policy consistently enhances lifetime energy gen-

611 eration, reduces efficiency losses, and adapts more effectively to changing hydrologic con-  
 612 ditions. These results demonstrate that proactive, flow-informed turbine management  
 613 enables smoother adaptation to evolving water regimes and provides sustained perfor-  
 614 mance gains under future uncertainty.

615 The HyTUNE replacement strategy aligns closely with recent retrofitting efforts  
 616 at the Hoover Hydropower Plant. After 2000, reservoir levels declined sharply as drought  
 617 persisted and water demands increased. In response to lost capacity and reduced effi-  
 618 ciency, operators replaced five turbines with low-head models optimized for reduced wa-  
 619 ter levels, lowering the design head from 150 m to 138 m and increasing discharge ca-  
 620 pacity by 20 %. HyTUNE recommends a similar approach, increasing discharge capaci-  
 621 ty by 20 % while reducing the design head to 138.75 m in anticipation of projected in-  
 622 flow variability, illustrating how adaptive strategies can reconcile long-term hydrologic  
 623 change with sustained generation performance. This agreement between model recom-  
 624 mendations and actual retrofitting actions at Hoover indicates that the decisions taken  
 625 there were technically well-founded and consistent with adaptive, performance-driven  
 626 planning.

#### 627 ***4.3.3 HyTUNE outperforms reactive approaches across all scenarios***

628 Figure 7 shows a comprehensive analysis of HyTUNE against the two benchmark  
 629 scenarios detailing how HyTUNE performance compares to the two benchmarks for dif-  
 630 ferent future climate characteristics and performance indicators. The top panels com-  
 631 pare the  $RA_1$  with the OPT from HyTUNE, while the bottom panels compare the  $RA_2$   
 632 with the same OPT. The accompanying bar plots show the total number of turbines re-  
 633 placed under each strategy throughout the simulation period. Notably, OPT recommends  
 634 different numbers of replacement phases (four or five) depending on system performance  
 635 and prevailing hydrologic conditions. Each line in the parallel coordinate plot represents  
 636 a single climate scenario, showing relationships among mean discharge ( $Q_{\text{mean}}$  in  $\text{m}^3/\text{s}$ ),  
 637 the 10th percentile and coefficient of variation of reservoir level ( $RL_{10}$  in m,  $RL_{CV}$ ), drought  
 638 frequency ( $Fr_{\text{drought}}$ ) that measures the fraction of time reservoir discharge falls below  
 639  $300 \text{ m}^3/\text{s}$ . The color of each line in both panels corresponds to its  $\Delta\text{NPV}$  value, where  
 640 lighter tones indicate lower  $\Delta\text{NPV}$  and darker tones indicate higher  $\Delta\text{NPV}$ . While we  
 641 optimize HyTUNE performance to maximize NPV, we also benchmark the produced strate-  
 642 gies against other important performance metrics that are not directly used in calibra-

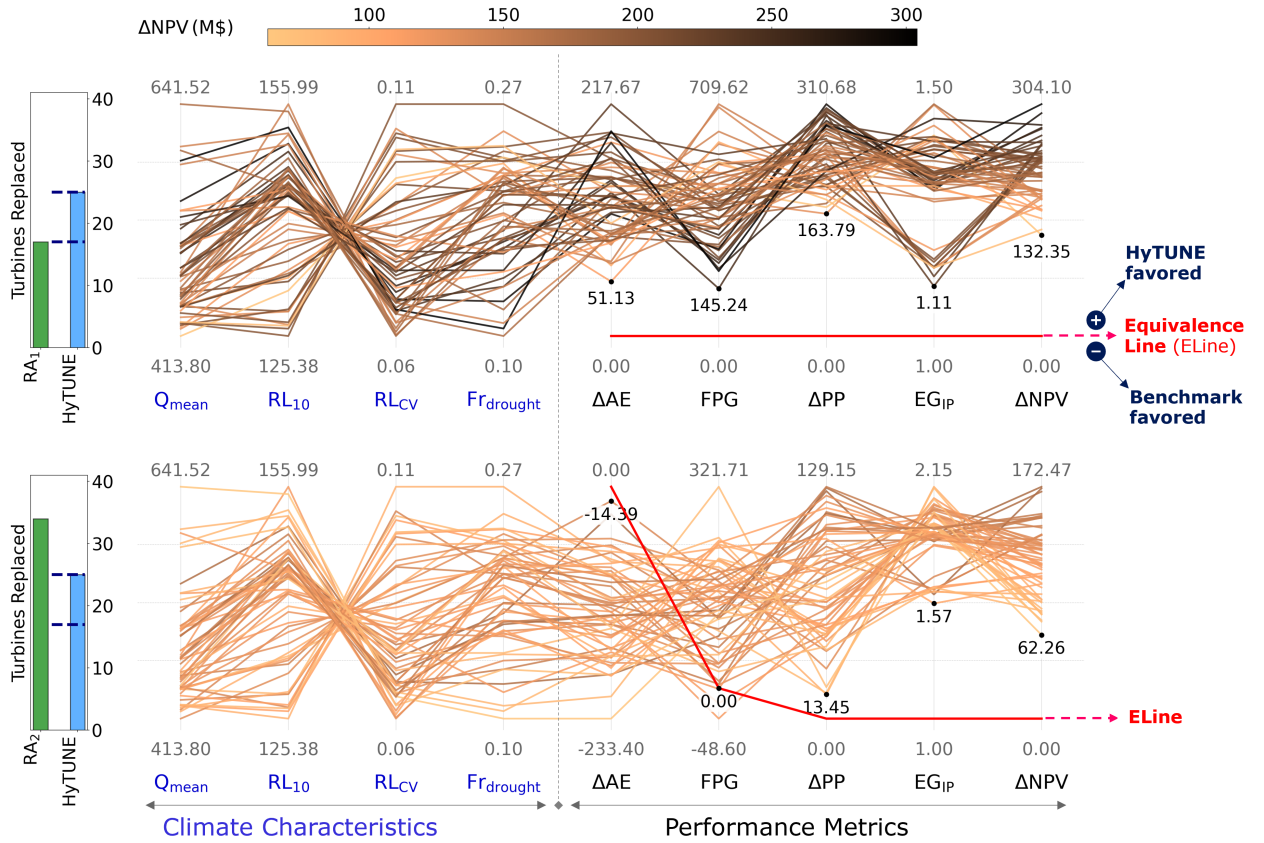


Figure 7: Parallel coordinate plots comparing scenario characteristics and retrofit strategies. The top panels contrast the one-time reactive replacement strategy (RA<sub>1</sub>) with the optimized policy tree (OPT) from HyTUNE, and the bottom panels compare the two-time reactive replacement strategy (RA<sub>2</sub>) with the same OPT. Each line represents an individual inflow scenario. Scenario characteristics (blue labels) include mean discharge (Q<sub>mean</sub>), the 10th percentile and coefficient of variation of reservoir level (RL<sub>10</sub>, RL<sub>cv</sub>), and drought frequency (Fr<sub>drought</sub>). Performance metrics (black labels) include the change in annual energy generation relative to the reactive cases (ΔAE), firm power gain (FPG), change in peak energy generation relative to the reactive cases (ΔPP), and energy generation per installed power (EG<sub>IP</sub>). The final axis shows the change in net present value relative to the reactive cases (ΔNPV). Line colors represent ΔNPV, illustrating trade-offs among hydrologic and operational outcomes. Left-side bar plots compare the total number of turbines replaced under the reactive (green) and HyTUNE (blue) strategies. The red line on both panels marks performance equivalence; scenarios above the line indicate HyTUNE performs better, while those below indicate the benchmark performs better.

643 tion. These include the change in annual average energy generation (ΔAAE in GWh),  
 644 firm power gain (FPG in MWh/day), change in peak-period energy generation (ΔPP  
 645 in GWh/year), EG<sub>IP</sub>, energy generated per installed capacity, and change in net present  
 646 value (ΔNPV in M\$). The red line denotes performance equivalence; scenarios above it

647 reflect higher HyTUNE performance, while those below reflect higher benchmark per-  
648 formance.

649 In the top-right bar plot, the reactive strategy (green) replaces all 17 turbines si-  
650 multaneously at mid-life, whereas the optimized approach (blue) replaces 23 or 29 tur-  
651 bines selectively over time. Across all performance metrics, scenarios that fall above the  
652 equivalence line indicate higher HyTUNE performance compared with RA<sub>1</sub>, even with-  
653 out considering specific climate characteristics. HyTUNE produces more energy, with  
654 annual gains ranging from 51 to 217 GWh and firm energy increases between 145 and  
655 709 MWh/d. The mean peak-period energy generation gain ( $\Delta PP$ ) ranges from 163 to  
656 310 GWh/y, demonstrating how the optimized policy enhances peak capacity and bet-  
657 ter meets peak grid demand. This targeted replacement schedule improves overall effi-  
658 ciency. Despite requiring additional replacements (six or twelve units), HyTUNE uses  
659 the total installed capacity more effectively, as indicated by the  $EG_{IP}$  ratio remaining  
660 near 1.1 for twelve additional units and 1.5 for six, along with higher  $\Delta AE$  values.

661 These gains translate into greater economic feasibility and stronger returns. Hy-  
662 TUNE achieves a better NPV across all future climates, the benefits are largest for sce-  
663 narios with higher discharges ( $Q_{\text{mean}}$ ), reservoir elevations ( $RL_{10}$ ) and fewer droughts  
664 ( $Fr_{\text{drought}}$ ). In contrast, scenarios with lower  $Q_{\text{mean}}$  and  $RL_{10}$  and higher  $RL_{CV}$  exhibit  
665 greater FPG and  $EG_{IP}$  values, indicating that HyTUNE increases reliability by raising  
666 firm power and operating more efficiently under drier and more variable hydrologic con-  
667 ditions. In other words, the reactive approach (RA<sub>1</sub>) performs worse under dry and highly  
668 variable hydrologic futures.

669 The bottom panels compare the two-time reactive replacement strategy (RA<sub>2</sub>), which  
670 replaces all turbines twice after 40 and 80 years of operation, with the optimized pol-  
671 icy (OPT) from HyTUNE. In this case, HyTUNE replaces 5 to 11 fewer turbines but does  
672 so gradually rather than through two bulk replacement cycles. Although RA<sub>2</sub> achieves  
673 higher total energy production due to its larger number of new turbines, the  $\Delta AE$  val-  
674 ues narrow under dry and highly variable futures, indicating that HyTUNE delivers com-  
675 parable energy output despite fewer replacements. HyTUNE increases firm energy gain  
676 in more than 95 % of scenarios and outperforms RA<sub>2</sub> across nearly all other performance  
677 metrics. The mean peak-period energy generation gain ( $\Delta PP$ ) ranges from 13 to 129 GWh/y,  
678 demonstrating enhanced peak capacity and improved alignment with grid demand. The

679 minimum EGIP ratio exceeding 1.5 further confirms that the optimized policy achieves  
680 superior operational efficiency compared with RA<sub>2</sub>.  $\Delta$ NPV for HyTUNE increases by  
681 62–172 M \$, underscoring the economic advantage of adaptive planning. These results  
682 show that adaptive scheduling sustains reliable generation more efficiently than repet-  
683 itive, full-fleet replacements. scheduling sustains reliable generation more efficiently than  
684 repetitive, full-fleet replacements. Similar to the RA<sub>1</sub> comparison, scenarios with lower  
685  $Q_{\text{mean}}$  and RL<sub>10</sub> and higher RL<sub>CV</sub> show higher FPG values, indicating that HyTUNE  
686 increases reliability under such conditions.

## 687 **5 Limitations and Future work**

688 This study has several limitations that also point to directions for future work. Al-  
689 though HyTUNE is broadly applicable to hydropower retrofitting, it was demonstrated  
690 through a single case study. Future research will test HyTUNE’s potential across diverse  
691 climatic, socio-economic, and regulatory conditions. A key extension is to couple HyTUNE  
692 with basin-scale water resources models so it can represent the coordinated operation  
693 of hydropower plants within larger water systems. This expansion will increase compu-  
694 tational demands, because a replacement decision at one facility can alter flows, constraints,  
695 and dispatch opportunities at others. At the same time, such expansion would create op-  
696 portunities to coordinate operations, reduce exposure to future variability, and sustain  
697 efficient performance across entire river basins.

698 Similarly, Hydropower will play an important role in future low carbon systems.  
699 As power systems incorporate more renewable generation such as wind and solar, hy-  
700 dropower will shift from prioritizing energy production to providing flexibility and bal-  
701 ancing variable renewable generation. Extending HyTUNE to account for ancillary ser-  
702 vices will allow the framework to capture these emerging operational roles. This capa-  
703 bility can be achieved by coupling HyTUNE with power system models, which would link  
704 water system optimization with grid dynamics and market evolution. Such integration  
705 would create a unified planning tool that aligns plant level modernization with power  
706 system needs while retaining HyTUNE’s core functionality for turbine evaluation. It will  
707 also allow HyTUNE to produce turbine replacement policies that are responsive to chang-  
708 ing electricity prices, in addition to changing hydrology.

709 The Hoover Hydropower Plant, selected as a case study, is a key facility for U.S.  
710 power production and highlights the risks that changing hydrology poses to hydropower  
711 infrastructure. It also introduces unique modeling challenges. Hoover’s release policies  
712 are revised frequently and depend primarily on demand rather than reservoir storage,  
713 which adds uncertainty when extrapolating historical behavior into future conditions.  
714 In contrast, most reservoirs follow rule curves that remain more consistent over time and  
715 are therefore easier to project. Inflow scenarios introduce an additional limitation. The  
716 mean flow of the projected scenarios does not match historical conditions after 2004 when  
717 compared with observations. This mismatch reflects constraints in the calibration pe-  
718 riod. Representing inflow to Hoover is therefore challenging, yet the conceptual approach  
719 and resulting performance insights remain robust.

720 Relicensing introduces an additional consideration for hydropower plants, includ-  
721 ing those in the United States. Major retrofits often coincide with relicensing cycles, and  
722 many owners evaluate turbine replacement and/or capacity upgrades as part of this pro-  
723 cess (A. L. Levine et al., 2017; IHA, 2022). These regulatory milestones can accelerate  
724 or delay modernization actions independent of hydrologic or economic drivers. HyTUNE  
725 does not currently represent relicensing constraints, so future work should incorporate  
726 regulatory timing and compliance requirements to improve alignment with real decision  
727 processes. Future applications should also prioritize plants approaching relicensing, as  
728 nearly 30 percent of U.S. hydropower projects will enter relicensing within the next decade  
729 (Russo, 2021), and modernization decisions are most likely to occur during these peri-  
730 ods.

731 The current version of HyTUNE generates strategies that maximize net present value  
732 while improving firm power, peak capacity, and operational efficiency. These results demon-  
733 strate strong potential to enhance economic and technical performance under uncertainty.  
734 Future extensions could expand the framework to explore alternative operating objec-  
735 tives, including maximizing hydropeaking capacity or capacity factor, which helps iden-  
736 tify designs that remain efficient under emerging flow variability and shifting system re-  
737 quirements. Additional extensions could improve efficiency at low flows or support eco-  
738 logical releases during periods of reduced water availability. These enhancements would  
739 broaden the relevance of HyTUNE across diverse hydrologic and operational contexts  
740 while retaining its core strength as a decision tool for turbine modernization.

Overall, HyTUNE has strong potential for extension. The framework provides a flexible and modular structure that can support new case studies, additional turbine types such as Kaplan and Pelton, emerging technologies including fish friendly and variable speed designs, and repair oriented cost models. These extensions are valuable because (i) different turbine types and technologies can outperform existing configurations under specific hydrologic or operational conditions, and (ii) component level repair costs or partial rehabilitation options can be incorporated into the policy tree to evaluate their economic and operational value alongside full replacement. New replacement policies can be generated for any site by substituting local data on hydrology, reservoir operations, or turbine characteristics. New actions, thresholds, and triggers can also be added as project priorities evolve, allowing HyTUNE to align with diverse site specific objectives.

## 6 Discussion and conclusions

The results of this study highlight both the scale of the hydropower modernization challenge and the opportunities for adaptive planning. Turbine retrofitting remains understudied in the water resources literature, where they are often treated as stable components that perform consistently regardless of changing conditions. Climate variability and evolving grid demands now place increasing pressure on their efficiency and flexibility. These trends underscore the need for models that link long term investment decisions with hydrologic and operational change. We therefore frame the discussion in two parts. First, we assess national patterns in turbine aging to quantify the modernization gap. Second, we argue how HyTUNE supports resilient turbine planning through adaptive optimization and flexible integration with hydrologic information.

### 6.1 In the US, turbine aging significantly outpaces replacement

Across the U.S., 2252 hydropower plants with approximately 5100 turbines have an installed capacity of 80.58 GW (Uría-Martínez & Johnson, 2023). In 2022, these facilities generated 28.7 % of the nation’s renewable electricity and 6.2 % of its total electricity, making HP a key component of the US energy mix.

In this section, we present an overview of the condition of the national hydropower fleet by combining turbine-level data from the Existing Hydropower Assets (EHA) database (M. Johnson et al., 2023) with system-level replacement statistics from the U.S. Hydropower

771 Market Report (HMR) (Uría-Martínez et al., 2022). Merging these datasets allowed us  
 772 to reconstruct the evolution of average turbine age from 1990 to 2024 with its associated  
 773 uncertainty arising from incomplete replacement records (Figure 8).

774 To analyze turbine aging patterns, we extracted the commissioning year of each  
 775 unit from the EHA database. These data were used to produce the “no replacement” curve  
 776 in Figure 8, which shows how the national fleet would age if no replacements occurred.  
 777 The blue curve (“with recorded replacements”) resets turbine age at each documented  
 778 replacement event, yielding a more realistic estimate of the fleet’s age distribution. To  
 779 account for replacements, we used unit-level replacement years from the EHA database  
 780 and integrated aggregate statistics from the HMR, which report the total number of tur-  
 781 bines replaced between 2007 and 2022 but do not specify which units or plants were in-  
 782 volved. Because the two datasets differ in the number of reported replacements and the  
 783 HMR lacks unit-level attribution, we assumed a replacement age of 55 years and assigned  
 784 each inferred replacement to units that would have reached that age during the reported  
 785 period (i.e., commissioning year = 2020 – 55). This combined dataset provides a com-  
 786 prehensive reconstruction of the historical evolution of the U.S. turbine fleet, capturing  
 both recorded and inferred replacement activity.

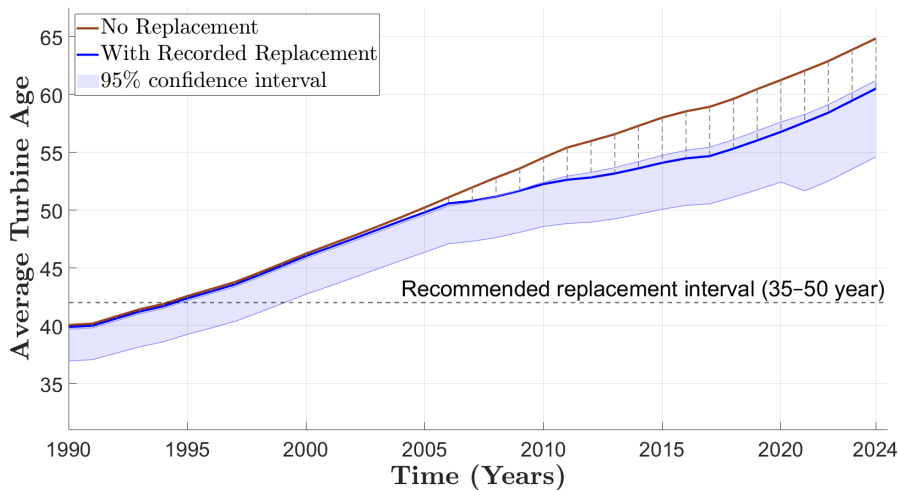


Figure 8: Average turbine age in the U.S. hydropower fleet (1990–2024). The brown line shows the average operational age, while the blue line accounts for recorded turbine replacements. The blue shaded band denotes the 95 % Monte Carlo interval derived from 2000 replacement scenarios. The dashed horizontal line indicates the manufacturer-recommended replacement range of 35–50 years.

787

788 Unit-level analysis of hydropower facilities in the Columbia and Colorado River basins  
789 indicates that up to 10 % of turbine replacement records are missing or inconsistently  
790 reported. To account for this data uncertainty, we developed a Monte Carlo framework  
791 that perturbs missing or inconsistent records. For turbines commissioned before 1990,  
792 the algorithm randomly replaces between 0% and 15% of units in each realization, as-  
793 signing replacement ages uniformly distributed between 30 and 70 years. The same life-  
794 time range randomizes the 2007–2022 aggregate adjustments, producing 5000 indepen-  
795 dent realizations. The 2.5<sup>t</sup> and 97.5<sup>t</sup> percentiles of the ensemble define the 95 % con-  
796 fidence interval (blue shaded region).

797 The small separation between the deterministic blue curve and its uncertainty band  
798 indicates that, although replacement data errors exist at the unit level, the fleet-average  
799 trend is robust. This figure reveals a concerning trend: the average turbine age is ris-  
800 ing steadily, indicating that replacements are not keeping pace with aging. The horizon-  
801 tal dashed line marks the manufacturer-recommended replacement window (35–50 years),  
802 serving as a benchmark for assessing modernization needs. By 2010, roughly half of U.S.  
803 turbines had exceeded the manufacturer-recommended replacement range of 35–50 years  
804 (Quaranta & Hunt, 2022), and the national mean has now surpassed 55 years. This grow-  
805 ing imbalance suggests that many turbines operate well beyond their intended lifespan,  
806 increasing risks of mechanical failure and efficiency loss. This persistent imbalance be-  
807 tween aging and replacement underscores the urgent need for proactive modernization  
808 strategies that safeguard reliability and sustain the long-term performance of the U.S.  
809 hydropower fleet.

## 810 **6.2 Adaptive optimization for turbine modernization and operational** 811 **resilience: The role of HyTUNE**

812 Modernizing hydropower plants has become essential as aging infrastructure, cli-  
813 mate variability, and changing grid demands reduce efficiency and operational flexibil-  
814 ity. Historically, expanding hydropower capacity relied on the construction of new dams  
815 and large civil works, but this hard-path approach is no longer viable given its environ-  
816 mental consequences. Modernization of existing plants now focuses on maintenance and  
817 life-extension programs (Mikhailov et al., 2021; Quaranta & Hunt, 2022). Although ex-  
818 tending turbine lifetimes can be beneficial, outdated designs often perform poorly un-  
819 der evolving hydrologic and grid conditions. Maintenance and rehabilitation should there-

820 fore include systematic assessments to determine when and how turbine replacement can  
821 improve efficiency and long-term value. Delayed or poorly informed modernization de-  
822 cisions risk decades of reduced generation efficiency, lost revenue, and declining reliabil-  
823 ity.

824 We introduce HyTUNE, a dynamic decision-support tool that integrates basin hy-  
825 drology, plant hydraulics, and adaptive optimization to guide turbine replacement tim-  
826 ing and configuration. HyTUNE applies dynamic planning to hydropower adaptation,  
827 formulating the retrofitting problem as a control problem with a flexible policy struc-  
828 ture. Retrofitting policies are represented as decision trees, where system indicators such  
829 as reservoir level or turbine efficiency trigger actions that include replacing turbines with  
830 new head and/or discharge models or deferring upgrades. This approach enables oper-  
831 ational decisions to evolve in response to observed hydrologic and performance changes,  
832 improving resilience under uncertainty.

833 Applied to the Hoover Hydropower Plant, HyTUNE generated adaptive operational  
834 policies that consistently outperformed conventional reactive strategies across a wide en-  
835 semble of hydrologic futures. Relative to two benchmark scenarios, the optimized ap-  
836 proach dynamically adapted turbine configurations (turbine design head and discharge  
837 capacity), as well as the number and timing of replacements, applying more frequent in-  
838 terventions in drier futures to manage rising variability in reservoir and inflow conditions.  
839 This strategy increased net present value, firm power, peak-period generation, and op-  
840 erational efficiency, even though one benchmark scenario replaced more than 30 % more  
841 turbines. The framework maintained strong performance without explicit conditioning  
842 on specific climate scenarios. Climate variability still influenced outcomes; economic gains  
843 were greatest under wetter conditions with higher outflows and fewer droughts, whereas  
844 improvements in firm power were most pronounced under drier conditions.

845 HyTUNE and its optimization framework provide a flexible foundation for turbine  
846 planning under evolving hydrologic and operational conditions. The framework is gen-  
847 eralizable. It can use inflow projections developed at grid scale, such as recent continen-  
848 tal datasets (Broman et al., 2024), or plant level inflow estimates and high resolution reser-  
849 voir operation models. It also accommodates data driven representations of operating  
850 behavior, including the LSTM model employed here. This flexibility allows the frame-  
851 work to support large scale power system planning, which requires reliable insight into

852 future hydropower generation and capacity. It also enables site specific assessments that  
853 capture the detailed behavior of individual plants. Together, these elements help bridge  
854 the gap between long term power system studies and the operational realities that shape  
855 hydropower performance.

856 Although proprietary retrofit models exist within the hydropower industry, their  
857 structure and capabilities are not publicly documented. HyTUNE provides an open and  
858 transparent platform that supports systematic exploration of turbine retrofitting. This  
859 capability enables resource adequacy studies to revisit the common assumption of fixed  
860 hydropower performance over 10 to 20 year horizons and allows reliability studies to eval-  
861 uate how changes in turbine technologies influence system flexibility and resilience. New  
862 turbine designs, modernization strategies, and operational pathways can therefore be as-  
863 sessed consistently across water and energy domains.

864 Together, these features position HyTUNE as a practical tool for hydropower mod-  
865 ernization in a changing world. Its adaptive structure supports continuous decision mak-  
866 ing as hydrologic, economic, and policy conditions evolve. By enabling direct coupling  
867 with future inflow projections, evaluating multiple turbine configurations, and interfac-  
868 ing with power system models, HyTUNE bridges plant scale modernization with system  
869 scale planning and helps align long lived investment decisions with the operational re-  
870 alities that shape hydropower performance over time.

## 871 **7 Data Availability Statement**

872 The HyTUNE model and data used in this study are openly available through the  
873 Zenodo repository (Yildiz et al., 2025b) at <https://doi.org/10.5281/zenodo.18058173>.  
874 The repository includes the complete HyTUNE implementation, all input datasets, and  
875 two Jupyter notebooks: one for decision-tree optimization and one for scenario-based sim-  
876 ulation and post-processing. Together, these resources enable full reproduction of the  
877 HyTUNE simulations and figures presented in this paper.

## 878 **Acknowledgments**

879 We thank Oak Ridge National Laboratory for providing access to the Baseline Cost Model  
880 for U.S. hydropower projects, which informed the turbine retrofit cost analysis in this  
881 study. We acknowledge the use of regulated flow projections produced under the U.S.

882 Department of Energy Water Power Technologies Office's SECURE Water Act Section  
883 9505 Assessment (9505 project).

884 **References**

- 885 Abboud, H., Baker, E., Baiotto, T., Weigand, C., & Quinn, J. (2022). Optimizing  
886 for water equity in the colorado river basin. In *2022 systems and information  
887 engineering design symposium (sieds)* (pp. 190–195).
- 888 Al-Hardanee, O. F., & Demirel, H. (2024). Hydropower station status prediction us-  
889 ing rnn and lstm algorithms for fault detection. *Energies*, *17*(22), 5599.
- 890 Amougou, C. B., Tsuanyo, D., Fioriti, D., Kenfack, J., Aziz, A., & Elé Abiama,  
891 P. (2022). Lcoe-based optimization for the design of small run-of-river hy-  
892 dropower plants. *Energies*, *15*(20), 7507.
- 893 Arnold, W., Giuliani, M., & Castelletti, A. (2024). Floating photovoltaics may re-  
894 duce the risk of hydro-dominated energy development in africa. *Nature Energy*,  
895 1–10.
- 896 Barzola-Monteses, J., Gomez-Romero, J., Espinoza-Andaluz, M., & Fajardo, W.  
897 (2022). Hydropower production prediction using artificial neural networks:  
898 an ecuadorian application case. *Neural Computing and Applications*, *34*(16),  
899 13253–13266.
- 900 Bisnett, R., Grossmann, N., Andrews, T., Milanowicz, D., & Maas, H. (2022). Red  
901 rock hydroelectric project–new hydro development at an existing flood control  
902 dam. In *E3s web of conferences* (Vol. 346, p. 04006).
- 903 Broman, D., & Voisin, N. (2025, June). *Cmip6-based mosartwmpy simula-*  
904 *tions (inflow, storage, release) for conus multi-use reservoirs.* Zenodo.  
905 Retrieved from <https://doi.org/10.5281/zenodo.15611029> doi:  
906 10.5281/zenodo.15611029
- 907 Broman, D., Voisin, N., Kao, S.-C., Fernandez, A., & Ghimire, G. R. (2024). Multi-  
908 scale impacts of climate change on hydropower for long-term water-energy  
909 planning in the contiguous united states. *Environmental Research Letters*,  
910 *19*(9), 094057.
- 911 Brown, S., Yildiz, V., & Rougé, C. (2024, April). Modernising RoR Hydropower: A  
912 Study on Retrofitting Aged Turbines for Optimal Performance. In *Egu general  
913 assembly conference abstracts* (p. 9612). doi: 10.5194/egusphere-egu24-9612
- 914 Cameron, A., & Pracheil, B. (2022). *Environmental flow requirements from ferc*  
915 *licenses across the us* (Tech. Rep.). Oak Ridge National Lab.(ORNL), Oak  
916 Ridge, TN (United States). Retrieved from <https://hydrosource.ornl.gov/>

- 917 `data/datasets/ornl-environmental-flow-requirements/`
- 918 Carlino, A., Wildemeersch, M., Chawanda, C. J., Giuliani, M., Sterl, S., Thiery,  
919 W., ... Castelletti, A. (2023). Declining cost of renewables and climate  
920 change curb the need for african hydropower expansion. *Science*, *381*(6658),  
921 eadf5848.
- 922 Celebioglu, K., Altintas, B., Aradag, S., & Tascioglu, Y. (2017). Numerical research  
923 of cavitation on francis turbine runners. *International Journal of Hydrogen En-*  
924 *ergy*, *42*(28), 17771–17781.
- 925 Cheng, M., McCarl, B., & Fei, C. (2022). Climate change and livestock production:  
926 a literature review. *Atmosphere*, *13*(1), 140.
- 927 Cheng, Q., Liu, P., Feng, M., Cheng, L., Ming, B., Luo, X., ... Xia, J. (2023). Com-  
928plementary operation with wind and photovoltaic power induces the decrease  
929 in hydropower efficiency. *Applied Energy*, *339*, 121006.
- 930 Cohen, J. S., & Herman, J. D. (2021). Dynamic adaptation of water resources sys-  
931 tems under uncertainty by learning policy structure and indicators. *Water Re-*  
932 *sources Research*, *57*(11), e2021WR030433.
- 933 Datta, S., Somani, A., Alam, M. J. E., Sun, X., Fotedar, V., & Banicki, A. (2022).  
934 Changes in hydropower resource operations following participation in the caiso  
935 energy imbalance market-a case study. In *2022 ieee power & energy society*  
936 *general meeting (pesgm)* (pp. 1–5).
- 937 De Silva, T., Jorgenson, J., Macknick, J., Keohan, N., Miara, A., Jager, H., &  
938 Pracheil, B. (2022). Hydropower operation in future power grid with vari-  
939 ous renewable power integration. *Renewable Energy Focus*, *43*, 329–339.
- 940 Diaz, F. J., Contreras, J., Muñoz, J. I., & Pozo, D. (2010). Optimal scheduling of a  
941 price-taker cascaded reservoir system in a pool-based electricity market. *IEEE*  
942 *Transactions on Power Systems*, *26*(2), 604–615.
- 943 Dorji, U., & Ghomashchi, R. (2014). Hydro turbine failure mechanisms: An  
944 overview. *Engineering Failure Analysis*, *44*, 136–147.
- 945 Egré, D., & Milewski, J. C. (2002). The diversity of hydropower projects. *Energy*  
946 *Policy*, *30*(14), 1225–1230.
- 947 EIA. (2025, March). *Electricity monthly update: Wholesale electricity markets*.  
948 Retrieved from [https://www.eia.gov/electricity/monthly/update/](https://www.eia.gov/electricity/monthly/update/wholesale-markets.php)  
949 `wholesale-markets.php` (Accessed May 4, 2025)

- 950 Emmanuel, M., Doubleday, K., Cakir, B., Marković, M., & Hodge, B.-M. (2020). A  
951 review of power system planning and operational models for flexibility assess-  
952 ment in high solar energy penetration scenarios. *Solar Energy*, *210*, 169–180.
- 953 ESHA. (2004). Guide on how to develop a small hydropower plant [Computer soft-  
954 ware manual].
- 955 Fakhfakh, R., Ammar, A. B., & Amar, C. B. (2017). Deep learning-based recom-  
956 mendation: Current issues and challenges. *International Journal of Advanced*  
957 *Computer Science and Applications*, *8*(112).
- 958 Fälth, H. E., Hedenus, F., Reichenberg, L., & Mattsson, N. (2025). Through energy  
959 droughts: hydropower’s ability to sustain a high output. *Renewable and Sus-*  
960 *tainable Energy Reviews*, *214*, 115519.
- 961 Fälth, H. E., Mattsson, N., Reichenberg, L., & Hedenus, F. (2023). Trade-offs  
962 between aggregated and turbine-level representations of hydropower in opti-  
963 mization models. *Renewable and Sustainable Energy Reviews*, *183*, 113406.
- 964 Farmer, M. (2020, August 7). The past, present, and future of maintenance at  
965 the hoover dam. *Power Technology*. Retrieved from [https://www.power-  
966 -technology.com/features/hoover-dam-maintenance-covid-19-hydro-  
967 -generation-lake-mead-climate-change-post-apocalypse/](https://www.power-technology.com/features/hoover-dam-maintenance-covid-19-hydro-generation-lake-mead-climate-change-post-apocalypse/)
- 968 Feng, Z.-k., Luo, T., Niu, W.-j., Yang, T., & Wang, W.-c. (2023). A lstm-based  
969 approximate dynamic programming method for hydropower reservoir operation  
970 optimization. *Journal of Hydrology*, *625*, 130018.
- 971 FERC. (2024, March). *2023 state of the markets report* (Tech. Rep.). Federal En-  
972 ergy Regulatory Commission. Retrieved from [https://www.ferc.gov/sites/  
973 default/files/2024-03/24\\_State-of-the-market\\_0320\\_1715.pdf](https://www.ferc.gov/sites/default/files/2024-03/24_State-of-the-market_0320_1715.pdf) (FERC  
974 Staff Report, Office of Energy Policy and Innovation)
- 975 Fleck, J., & Castle, A. (2022). Green light for adaptive policies on the colorado  
976 river. *Water*, *14*(1). Retrieved from [https://www.mdpi.com/2073-4441/14/  
977 1/2](https://www.mdpi.com/2073-4441/14/1/2) doi: 10.3390/w14010002
- 978 Fletcher, S., Lickley, M., & Strzepek, K. (2019). Learning about climate change  
979 uncertainty enables flexible water infrastructure planning. *Nature communica-*  
980 *tions*, *10*(1), 1782.
- 981 Fletcher, S. M., Miotti, M., Swaminathan, J., Klemun, M. M., Strzepek, K., & Sid-  
982 diqi, A. (2017). Water supply infrastructure planning: Decision-making frame-

- 983 work to classify multiple uncertainties and evaluate flexible design. *Journal of*  
984 *Water Resources Planning and Management*, 143(10), 04017061.
- 985 Garrett, K. P., McManamay, R. A., & Witt, A. (2023). Harnessing the power of en-  
986 vironmental flows: Sustaining river ecosystem integrity while increasing energy  
987 potential at hydropower dams. *Renewable and sustainable energy reviews*, 173,  
988 113049.
- 989 Gernaat, D. E., de Boer, H. S., Daioglou, V., Yalaw, S. G., Müller, C., & van Vu-  
990 uren, D. P. (2021). Climate change impacts on renewable energy supply.  
991 *Nature climate change*, 11(2), 119–125.
- 992 Goldberg, J., & Lier, O. E. (2011). *Rehabilitation of hydropower: an introduction to*  
993 *economic and technical issues*. World Bank, Washington, DC.
- 994 Hannoun, D., & Tietjen, T. (2023). Lake management under severe drought: lake  
995 mead, nevada/arizona. *JAWRA Journal of the American Water Resources As-*  
996 *sociation*, 59(2), 416–428.
- 997 Hassan, Q., Viktor, P., Al-Musawi, T. J., Ali, B. M., Algburi, S., Alzoubi, H. M.,  
998 ... Jaszczur, M. (2024). The renewable energy role in the global energy  
999 transformations. *Renewable Energy Focus*, 48, 100545.
- 1000 Herman, J. D., Quinn, J. D., Steinschneider, S., Giuliani, M., & Fletcher, S. (2020).  
1001 Climate adaptation as a control problem: Review and perspectives on dynamic  
1002 water resources planning under uncertainty. *Water Resources Research*, 56(2),  
1003 e24389.
- 1004 Hertwich, E., de Larderel, J. A., Arvesen, A., Bayer, P., Bergesen, J., Bouman, E.,  
1005 ... Suh, S. (2016). *Green energy choices: The benefits, risks, and trade-offs of*  
1006 *low-carbon technologies for electricity production*. Report of the International  
1007 Resource Panel, United Nations Environment Program (UNEP).
- 1008 Huang, Z., Yuan, X., & Liu, X. (2021). The key drivers for the changes in global wa-  
1009 ter scarcity: Water withdrawal versus water availability. *Journal of Hydrology*,  
1010 601, 126658.
- 1011 Hui, R., Herman, J., Lund, J., & Madani, K. (2018). Adaptive water infrastructure  
1012 planning for nonstationary hydrology. *Advances in Water Resources*, 118, 83–  
1013 94.
- 1014 Huizar, L., Díaz, S., Lansley, K., & Arnold, R. (2024). Economic impacts of the 2019  
1015 drought contingency plan in the lower colorado river basin: Water, energy, and

- 1016 recreation. *Journal of Environmental Engineering*, 150(4), 04024004.
- 1017 IHA, I. H. A. (2022). *Modernisation of hydropower*. IHA Factsheet. Retrieved from  
 1018 <https://www.hydropower.org/factsheets/modernisation> (Accessed: 2025-  
 1019 12-07)
- 1020 International Energy Agency. (2021). *Hydropower special market report: Analy-*  
 1021 *sis and forecast to 2030*. Paris: International Energy Agency. Retrieved from  
 1022 <https://www.iea.org/reports/hydropower-special-market-report> (Li-  
 1023 cence: CC BY 4.0)
- 1024 IRENA. (2012, June). *Renewable energy cost analysis: Hydropower* (Tech.  
 1025 Rep. Nos. Volume 1: Power Sector, Issue 3/5). Bonn, Germany: Inter-  
 1026 national Renewable Energy Agency (IRENA). Retrieved from [https://](https://www.irena.org/-/media/Files/IRENA/Agency/Publication/2012/RE_Technologies_Cost_Analysis-HYDROPOWER.pdf)  
 1027 [www.irena.org/-/media/Files/IRENA/Agency/Publication/2012/](https://www.irena.org/-/media/Files/IRENA/Agency/Publication/2012/RE_Technologies_Cost_Analysis-HYDROPOWER.pdf)  
 1028 [RE\\_Technologies\\_Cost\\_Analysis-HYDROPOWER.pdf](https://www.irena.org/-/media/Files/IRENA/Agency/Publication/2012/RE_Technologies_Cost_Analysis-HYDROPOWER.pdf) (Prepared by the  
 1029 IRENA Secretariat; internal review and external contributions acknowledged)
- 1030 Jenkin, T. J., Feldman, D. J., Kwan, A., & Walker, B. J. (2019). *Estimating the*  
 1031 *impact of residual value for electricity generation plants on capital recovery,*  
 1032 *levelized cost of energy, and cost to consumers* (Tech. Rep.). Golden, CO  
 1033 (United States): National Renewable Energy Lab.(NREL).
- 1034 Johnson, M., Kao, S.-C., & Uria-Martinez, R. (2023). *Existing hydropower as-*  
 1035 *sets unit dataset fy23* (Tech. Rep.). Oak Ridge National Lab.(ORNL), Oak  
 1036 Ridge, TN (United States). Retrieved from [https://doi.org/10.21951/](https://doi.org/10.21951/EHA_FY2024/2344935)  
 1037 [EHA\\_FY2024/2344935](https://doi.org/10.21951/EHA_FY2024/2344935)
- 1038 Johnson, M. M. (2024). *Existing hydropower assets (eha) capacity factor plant*  
 1039 *database, 2005–2023* (Tech. Rep.). Oak Ridge, Tennessee, USA: Oak Ridge  
 1040 National Laboratory. Retrieved from [https://hydrosource.ornl.gov/](https://hydrosource.ornl.gov/data/datasets/existing-hydropower-assets-eha-capacity-factor-plant-database-2005-2023/)  
 1041 [data/datasets/existing-hydropower-assets-eha-capacity-factor-plant](https://hydrosource.ornl.gov/data/datasets/existing-hydropower-assets-eha-capacity-factor-plant-database-2005-2023/)  
 1042 [-database-2005-2023/](https://hydrosource.ornl.gov/data/datasets/existing-hydropower-assets-eha-capacity-factor-plant-database-2005-2023/) (HydroSource) doi: 10.21951/EHA\_CapacityFactor  
 1043 [\\_FY2024/2406172](https://hydrosource.ornl.gov/data/datasets/existing-hydropower-assets-eha-capacity-factor-plant-database-2005-2023/)
- 1044 Kao, S.-C., Ashfaq, M., Rastogi, D., & Gangrade, S. (2022a). C mip6-based multi-  
 1045 model hydroclimate projection over the conterminous us. *HydroSource*. Oak  
 1046 Ridge National Laboratory, Oak Ridge, Tennessee, USA. DOI: [https://doi.](https://doi.org/10.21951/SWA9505V3/1887469)  
 1047 [org/10.21951/SWA9505V3/1887469](https://doi.org/10.21951/SWA9505V3/1887469).
- 1048 Kao, S.-C., Ashfaq, M., Rastogi, D., Gangrade, S., Uria Martinez, R., Fernan-

- 1049 dez, A., ... others (2022, 09). *The third assessment of the effects of cli-*  
1050 *mate change on federal hydropower* (Tech. Rep.). Oak Ridge National  
1051 Laboratory (ORNL), Oak Ridge, TN (United States). Retrieved from  
1052 <https://www.osti.gov/biblio/1887712> doi: 10.2172/1887712
- 1053 Kaunda, C. S., Kimambo, C. Z., & Nielsen, T. K. (2014). A technical discussion on  
1054 microhydropower technology and its turbines. *Renewable and Sustainable En-*  
1055 *ergy Reviews*, 35, 445–459.
- 1056 Kincic, S., Samaan, N., Datta, S., Somani, A., Yuan, H., Tan, J., ... Mosier, T. M.  
1057 (2022). *Hydropower modeling gaps in planning and operational studies* (Tech.  
1058 Rep.). WA (United States ...: Pacific Northwest National Laboratory  
1059 (PNNL), Richland.
- 1060 Kwakkel, J. H., Haasnoot, M., & Walker, W. E. (2016). Comparing robust decision-  
1061 making and dynamic adaptive policy pathways for model-based decision  
1062 support under deep uncertainty. *Environmental Modelling & Software*, 86,  
1063 168–183.
- 1064 Levine, A., Curtis, T., & Kazerooni, B. (2017, October). *Regulatory approaches*  
1065 *for adding capacity to existing hydropower facilities* (Technical Report No.  
1066 NREL/TP-6A20-70121). National Renewable Energy Laboratory. Re-  
1067 trieved from <https://docs.nrel.gov/docs/fy18osti/70121.pdf> doi:  
1068 10.2172/1391100
- 1069 Levine, A. L., Curtis, T. L., & Kazerooni, B. (2017). *Regulatory approaches for*  
1070 *adding capacity to existing hydropower facilities* (Tech. Rep.). Golden, CO,  
1071 USA: National Renewable Energy Laboratory.
- 1072 Liu, H., Brown, T., Andresen, G. B., Schlachtberger, D. P., & Greiner, M. (2019).  
1073 The role of hydro power, storage and transmission in the decarbonization of  
1074 the chinese power system. *Applied Energy*, 239, 1308–1321.
- 1075 Liu, L., He, G., Wu, M., Liu, G., Zhang, H., Chen, Y., ... Li, S. (2023). Climate  
1076 change impacts on planned supply–demand match in global wind and solar  
1077 energy systems. *Nature Energy*, 8(8), 870–880.
- 1078 Liu, X., Guo, S., Liu, P., Chen, L., & Li, X. (2011). Deriving optimal refill rules  
1079 for multi-purpose reservoir operation. *Water Resources Management*, 25, 431–  
1080 448.
- 1081 Liu, X., Luo, Y., Karney, B. W., & Wang, W. (2015). A selected literature review of

- 1082 efficiency improvements in hydraulic turbines. *Renewable and Sustainable En-*  
1083 *ergy Reviews*, 51, 18–28.
- 1084 Loucks, D. P., & Van Beek, E. (2017). *Water resource systems planning and man-*  
1085 *agement: An introduction to methods, models, and applications*. Springer.
- 1086 Lukas, J., & Payton, E. (2020). *Colorado river basin climate and hydrology: State of*  
1087 *the science* (Technical Report). Boulder, CO: Western Water Assessment, Co-  
1088 operative Institute for Research in Environmental Sciences. doi: 10.25810/3hcv  
1089 -w477
- 1090 March, P., & Jacobson, P. (2016, 07). Industry experience with power generation op-  
1091 tions for environmental flows..
- 1092 McCoy, A. L., Jacobs, K. L., Vano, J. A., Wilson, J. K., Martin, S., Pendergrass,  
1093 A. G., & Cifelli, R. (2022). The press and pulse of climate change: extreme  
1094 events in the colorado river basin. *JAWRA Journal of the American Water*  
1095 *Resources Association*, 58(6), 1076–1097.
- 1096 Mikhailov, V., Ivanchenko, I., & Prokopenko, A. (2021). Modern state of hy-  
1097 dropower and construction of hydro turbines in russia and abroad. *Thermal*  
1098 *Engineering*, 68, 83–93.
- 1099 Millstein, D., O’Shaughnessy, E., & Wiser, R. (2025). *Renewables and whole-*  
1100 *sale electricity prices (rewep) tool*. Retrieved from [https://emp.lbl.gov/](https://emp.lbl.gov/renewables-and-wholesale-electricity-prices-rewep)  
1101 [renewables-and-wholesale-electricity-prices-rewep](https://emp.lbl.gov/renewables-and-wholesale-electricity-prices-rewep) (Interactive vi-  
1102 sualization tool exploring trends in nodal wholesale energy pricing and their  
1103 relationship to wind and solar generation)
- 1104 Mishra, B. K., Kumar, P., Saraswat, C., Chakraborty, S., & Gautam, A. (2021).  
1105 Water security in a changing environment: Concept, challenges and solutions.  
1106 *Water*, 13(4), 490.
- 1107 Morgado, D., Troja, N., Kadyrzhanova, A., & Samuel, D. (2020). Hydropower mod-  
1108 ernization needs in asia. *no*, 1, 1–22.
- 1109 Muntean, S., Susan-Resiga, R., Göde, E., Baya, A., Terzi, R., & Tırşi, C. (2016).  
1110 Scenarios for refurbishment of a hydropower plant equipped with francis tur-  
1111 bines. *Renewable Energy and Environmental Sustainability*, 1, 30.
- 1112 Naz, B. S., Kao, S.-C., Ashfaq, M., Rastogi, D., Mei, R., & Bowling, L. C. (2016).  
1113 Regional hydrologic response to climate change in the conterminous united  
1114 states using high-resolution hydroclimate simulations. *Global and Planetary*

- 1115 *Change*, 143, 100–117.
- 1116 Neijens, B., & Hayes, C. (2017). Asset management partnership goes from  
1117 strength to strength after 15 years. *International Journal on Hydropower and*  
1118 *Dams, Issue Four*, 59–62. Retrieved from [https://go.copperleaf.com/](https://go.copperleaf.com/rs/727-PJA-841/images/Hydropower%26Dams_IssueFour_2017_Asset_Management_Partnership.PDF)  
1119 [rs/727-PJA-841/images/Hydropower%26Dams\\_IssueFour\\_2017\\_Asset](https://go.copperleaf.com/rs/727-PJA-841/images/Hydropower%26Dams_IssueFour_2017_Asset_Management_Partnership.PDF)  
1120 [\\_Management\\_Partnership.PDF](https://go.copperleaf.com/rs/727-PJA-841/images/Hydropower%26Dams_IssueFour_2017_Asset_Management_Partnership.PDF)
- 1121 O'Connor, P. W., DeNeale, S. T., Chalise, D. R., Centurion, E., & Maloof, A. (2015,  
1122 September). *Hydropower baseline cost modeling, version 2* (Tech. Rep. No.  
1123 ORNL/TM-2015/471). Oak Ridge, TN: Oak Ridge National Laboratory.  
1124 Retrieved from [https://info.ornl.gov/sites/publications/files/](https://info.ornl.gov/sites/publications/files/Pub58666.pdf)  
1125 [Pub58666.pdf](https://info.ornl.gov/sites/publications/files/Pub58666.pdf)
- 1126 Oladosu, G. A., & Ma, Y. (2025). *Baseline cost model for hydropower: Documen-*  
1127 *tation (2025)* (Tech. Rep. No. ORNL/TM-2025/3733). Oak Ridge, TN (United  
1128 States): Oak Ridge National Laboratory (ORNL).
- 1129 Owolabi, O. O., Lawson, K., Sengupta, S., Huang, Y., Wang, L., Shen, C., ...  
1130 Sunter, D. A. (2022). A robust statistical analysis of the role of hydropower  
1131 on the system electricity price and price volatility. *Environmental Research*  
1132 *Communications*, 4(7), 075003.
- 1133 Papillon, B., & Freeman, T. (2013). Rehabilitating the francis units at chief joseph.  
1134 *Hydr o Rev*, 32(8).
- 1135 Pei, Z., Rojas-Arevalo, A. M., de Haan, F. J., Lipovetzky, N., & Moallemi, E. A.  
1136 (2024). Reinforcement learning for decision-making under deep uncertainty.  
1137 *Journal of Environmental Management*, 359, 120968.
- 1138 Quaranta, E., Aggidis, G., Boes, R. M., Comoglio, C., De Michele, C., Patro, E. R.,  
1139 ... others (2021). Assessing the energy potential of modernizing the european  
1140 hydropower fleet. *Energy Conversion and Management*, 246, 114655.
- 1141 Quaranta, E., & Hunt, J. (2022). Retrofitting and refurbishment of hydropower  
1142 plants: Case studies and novel technologies. In *Renewable energy production*  
1143 *and distribution* (pp. 301–322). Elsevier.
- 1144 Ramião, J. P., Carvalho-Santos, C., Pinto, R., & Pascoal, C. (2023). Hydropower  
1145 contribution to the renewable energy transition under climate change. *Water*  
1146 *Resources Management*, 37(1), 175–191.
- 1147 Ramulifho, P., Ndou, E., Thifhulufhelwi, R., & Dalu, T. (2019). Challenges to imple-

- 1148 menting an environmental flow regime in the luvuvhu river catchment, south  
 1149 africa. *International Journal of Environmental Research and Public Health*,  
 1150 16(19). Retrieved from <https://www.mdpi.com/1660-4601/16/19/3694> doi:  
 1151 10.3390/ijerph16193694
- 1152 Rogers, J. D. (2010). Hoover dam: Operational milestones, lessons learned, and  
 1153 strategic import. In *Hoover dam: 75th anniversary history symposium* (pp.  
 1154 189–215).
- 1155 Russo, T. N. (2021). Rethinking low impact hydropower and renewable energy cer-  
 1156 tificates. *Climate and Energy*, 37(9), 26–32.
- 1157 Sample, J. E., Duncan, N., Ferguson, M., & Cooksley, S. (2015). Scotland’s hy-  
 1158 dropower: Current capacity, future potential and the possible impacts of cli-  
 1159 mate change. *Renewable and Sustainable Energy Reviews*, 52, 111–122.
- 1160 Santolin, A., Cavazzini, G., Pavesi, G., Ardizzon, G., & Rossetti, A. (2011). Techno-  
 1161 economical method for the capacity sizing of a small hydropower plant. *Energy*  
 1162 *Conversion and Management*, 52(7), 2533–2541.
- 1163 Schaeffer, R., Szklo, A. S., de Lucena, A. F. P., Borba, B. S. M. C., Nogueira,  
 1164 L. P. P., Fleming, F. P., . . . Boulahya, M. S. (2012). Energy sector vulner-  
 1165 ability to climate change: a review. *Energy*, 38(1), 1–12.
- 1166 Sensiba, C., & McCormick, E. (2021). Ferc regulatory considerations for  
 1167 project modifications. *Hydro Leader Magazine*. Retrieved from [https://](https://hydroleadermagazine.com/ferc-regulatory-considerations-for-project-modifications/)  
 1168 [hydroleadermagazine.com/ferc-regulatory-considerations-for-project-](https://hydroleadermagazine.com/ferc-regulatory-considerations-for-project-modifications/)  
 1169 [-modifications/](https://hydroleadermagazine.com/ferc-regulatory-considerations-for-project-modifications/) (Accessed: May 11, 2026)
- 1170 Shanbhag, V. V., Kandukuri, S. T., Olimstad, G., & Schlanbusch, R. (2025). Pre-  
 1171 dictive maintenance of critical components in hydroelectric turbines: A review.  
 1172 *IEEE Sensors Journal*.
- 1173 Singh, V. K., & Singal, S. K. (2017). Operation of hydro power plants-a review. *Re-*  
 1174 *newable and Sustainable Energy Reviews*, 69, 610–619.
- 1175 Smith, R., Zagona, E., Kasprzyk, J., Bonham, N., Alexander, E., Butler, A., . . .  
 1176 Jerla, C. (2022). Decision science can help address the challenges of long-term  
 1177 planning in the colorado river basin. *JAWRA Journal of the American Water*  
 1178 *Resources Association*, 58(5), 735–745.
- 1179 Smolarz, A., Lezhniuk, P., Kudrya, S., Komar, V., Lysiak, V., Hunko, I., . . .  
 1180 Orazbekov, Z. (2023). Increasing technical efficiency of renewable energy

- 1181 sources in power systems. *Energies*, *16*(6), 2828.
- 1182 Sternberg, R. (2010). Hydropower's future, the environment, and global electricity  
1183 systems. *Renewable and Sustainable Energy Reviews*, *14*(2), 713–723.
- 1184 Sun, J., Wang, Y., He, Y., Cui, W., Chao, Q., Shan, B., . . . Yang, X. (2024). The  
1185 energy security risk assessment of inefficient wind and solar resources under  
1186 carbon neutrality in china. *Applied Energy*, *360*, 122889.
- 1187 Thurber, T., Vernon, C., Sun, N., Turner, S., Yoon, J., & Voisin, N. (2021).  
1188 mosartwmpy: A python implementation of the mosart-wm coupled hydro-  
1189 logic routing and water management model. *Journal of Open Source Software*,  
1190 *6*(PNNL-SA-161232).
- 1191 Turner, S. W., Ghimire, G. R., Hansen, C., Singh, D., & Kao, S.-C. (2024). Hy-  
1192 dropower capacity factors trending down in the united states. *Nature Commu-  
1193 nications*, *15*(1), 5445.
- 1194 Turner, S. W., Voisin, N., & Nelson, K. (2022). Revised monthly energy genera-  
1195 tion estimates for 1,500 hydroelectric power plants in the united states. *Scien-  
1196 tific data*, *9*(1), 675.
- 1197 Tweed, K. (2013). Colorado river hydropower faces a dry future [news]. *IEEE Spec-  
1198 trum*, *50*(10), 14–15.
- 1199 Uría-Martínez, R., & Johnson, M. M. (2023). Us hydropower market report (2023  
1200 edition). *ORNL/SPR-2023/3076*, Oak Ridge National Laboratory.
- 1201 Uría-Martínez, R., White, D., Oladosu, G. A., DeSomber, K., & Johnson, M. M.  
1202 (2022). *Hydropower: Supply chain deep dive assessment* (Tech. Rep.). Oak  
1203 Ridge National Laboratory (ORNL), Oak Ridge, TN (United States). Re-  
1204 trieved from [https://www.energy.gov/sites/default/files/2024-12/  
1205 Hydropower%2520Supply%2520Chain%2520Report%2520-%2520Final%5B1%5D  
1206 .pdf](https://www.energy.gov/sites/default/files/2024-12/Hydropower%2520Supply%2520Chain%2520Report%2520-%2520Final%5B1%5D.pdf)
- 1207 USBR. (2011, March). *Hydropower resource assessment at existing reclamation fa-  
1208 cilities* (Tech. Rep.). U.S. Bureau of Reclamation. Retrieved from [https://  
1209 large.stanford.edu/courses/2016/ph240/lewis1/docs/USBRHydro.pdf](https://large.stanford.edu/courses/2016/ph240/lewis1/docs/USBRHydro.pdf)
- 1210 USBR. (2018). *Hydroelectric power – hoover dam*. Retrieved from [https://www  
1211 .usbr.gov/lc/hooverdam/faqs/powerfaq.html](https://www.usbr.gov/lc/hooverdam/faqs/powerfaq.html) (Accessed: 2025-04-18)
- 1212 Van Vliet, M. T., Sheffield, J., Wiberg, D., & Wood, E. F. (2016). Impacts of recent  
1213 drought and warm years on water resources and electricity supply worldwide.

- 1214 *Environmental Research Letters*, 11(12), 124021.
- 1215 Voisin, N., Hejazi, M. I., Leung, L. R., Liu, L., Huang, M., Li, H.-Y., & Tesfa, T.  
1216 (2017). Effects of spatially distributed sectoral water management on the re-  
1217 distribution of water resources in an integrated water model. *Water Resources*  
1218 *Research*, 53(5), 4253–4270.
- 1219 Voisin, N., Li, H., Ward, D., Huang, M., Wigmosta, M., & Leung, L. (2013). On an  
1220 improved sub-regional water resources management representation for integra-  
1221 tion into earth system models. *Hydrology and Earth System Sciences*, 17(9),  
1222 3605–3622.
- 1223 Wahl, T. L., & Cohen, E. A. (1999). Determination of controlled-release capac-  
1224 ity from trinity dam. In *1999 international water resources engineering confer-*  
1225 *ence*.
- 1226 Wang, Y., Xiao, Z., Liu, D., Chen, J., Liu, D., & Hu, X. (2022). Degradation trend  
1227 prediction of hydropower units based on a comprehensive deterioration index  
1228 and lstm. *Energies*, 15(17), 6273.
- 1229 Wheeler, K. G., Udall, B., Wang, J., Kuhn, E., Salehabadi, H., & Schmidt, J. C.  
1230 (2022). What will it take to stabilize the colorado river? *Science*, 377(6604),  
1231 373–375.
- 1232 Widén, Å., Renöfält, B. M., & Jansson, R. (2024). Environmental flows in a future  
1233 climate: Balancing hydropower production and ecosystem rehabilitation in the  
1234 ume river system, sweden. *Science of the Total Environment*, 955, 176622.
- 1235 Witt, A. M., Fernandez, A., Mobley, M. H., DeNeale, S., Bevelhimer, M., & Smith,  
1236 B. T. (2017). *How standard modular hydropower can enhance the environ-*  
1237 *mental, economic, and social benefits of new small hydropower development*  
1238 (Tech. Rep.). Oak Ridge, TN (United States): Oak Ridge National Laboratory  
1239 (ORNL).
- 1240 Yildiz, V., Brown, S., & Rougé, C. (2024). Importance of variable turbine efficiency  
1241 in run-of-river hydropower design under deep uncertainty. *Water Resources Re-*  
1242 *search*, 60(6), e2023WR035713.
- 1243 Yildiz, V., Brown, S., & Rougé, C. (2025a). Robust and computationally efficient  
1244 design for run-of-river hydropower. *Environmental Modelling & Software*, 183,  
1245 106220. Retrieved from [https://www.sciencedirect.com/science/article/](https://www.sciencedirect.com/science/article/pii/S1364815224002810)  
1246 [pii/S1364815224002810](https://www.sciencedirect.com/science/article/pii/S1364815224002810) doi: <https://doi.org/10.1016/j.envsoft.2024.106220>

- 1247 Yildiz, V., Hatipoglu, M. A., & Kumcu, S. Y. (2022). Climate change impacts on  
1248 water resources. In *Water and wastewater management: global problems and*  
1249 *measures* (pp. 17–25). Springer.
- 1250 Yildiz, V., & Vrugt, J. A. (2019). A toolbox for the optimal design of run-of-river  
1251 hydropower plants. *Environmental modelling & software*, *111*, 134–152. Re-  
1252 trieved from <https://doi.org/10.1016/j.envsoft.2018.08.018>
- 1253 Yildiz, V., Zaniolo, M., & Voisin, N. (2025b, December). *HyTUNE: Hytune v1.0.1*.  
1254 Zenodo [code]. Retrieved from <https://doi.org/10.5281/zenodo.18058173>  
1255 doi: 10.5281/zenodo.18058173
- 1256 Zaniolo, M., Fletcher, S., & Mauter, M. S. (2023). Multi-scale planning model for ro-  
1257 bust urban drought response. *Environmental Research Letters*, *18*(5), 054014.
- 1258 Zhang, D., Peng, Q., Lin, J., Wang, D., Liu, X., & Zhuang, J. (2019). Simulating  
1259 reservoir operation using a recurrent neural network algorithm. *Water*, *11*(4),  
1260 865.
- 1261 Zhou, Y., & Guo, S. (2013). Incorporating ecological requirement into multipur-  
1262 pose reservoir operating rule curves for adaptation to climate change. *Journal*  
1263 *of Hydrology*, *498*, 153–164.
- 1264 Zhou, Y., Hejazi, M., Smith, S., Edmonds, J., Li, H., Clarke, L., . . . Thomson, A.  
1265 (2015). A comprehensive view of global potential for hydro-generated electric-  
1266 ity. *Energy & Environmental Science*, *8*(9), 2622–2633.